IMAGE WATERMARKING

A thesis submitted to the faculty of Electrical Engineering Department, Military College of Signals, National University of Sciences and Technology, Pakistan, in partial fulfilment of the requirements for the degree of MS in Electrical Engineering

June, 2012

Muhammad Imran

Department of Electrical Engineering

Abstract

Watermarking is a possible solution for content authentication and copyright protection. Imperceptibility and robustness are two contradictory requirements for watermarking. In this thesis three approaches of watermarking to fulfill both the requirements are presented.

In the first approach a non-blind color image watermarking scheme using principle component analysis, discrete wavelet transform and singular value decomposition is proposed. The color components are uncorrelated using principle component analysis. The watermark is embedded into the singular values of discrete wavelet transformed sub-band associated with principle component containing most of the color information. In the second approach a robust color image watermarking scheme is proposed, in which a color watermark is embedded into a color image. Principle component analysis is used to un-correlate the R, G and B channels of both the images. Each channel of color watermark is embedded into singular values of corresponding channel of cover image after discrete wavelet decomposition. As original image is required at the time of extraction of watermark so given scheme is non-blind. In the third approach a robust gray image watermarking scheme based on human visual system is proposed. The perceptual quality of the watermarked image is controlled by determining adaptive scaling factor for each individual pixel value. To determine the adaptive scaling factor, human visual system (luminance masking, texture masking) and fuzzy inference systems were used.

Peak signal to noise ratio is used to measure the imperceptibility whereas similarity between original and extracted watermark is measured using normalized correlation coefficient. These schemes were tested against various attacks (including histogram equalization, rotation, Gaussian noise, scaling, cropping, JPEG compression, Y-shearing, X-shearing, median filtering, affine transformation, translation, sharpening, blurring, average filtering), to check the robustness. The results of proposed schemes are compared with state-of-the-art existing color watermarking schemes. The simulation results show that proposed schemes are robust and imperceptible, as compared to existing schemes.

Contents

List of Tables

List of Figures

Acknowledgements

I express my gratitude towards Allah Almighty with humility and humbleness, who helped me to complete MS.
I also thank my supervisor Dr. Abdul Ghafoor who apart from being an outstanding instructor has also proven to be a nice friend too. He was there to motivate and help me whenever an idea failed or whenever I was stuck during this research. His intellectual support throughout this research is invaluable. I am grateful to my thesis committee members including Dr. Imran Touqir, Dr. Adil Masood Siddique and Dr. Rizwan Ghaffar for their constant supervision and support. I am also grateful to administrative personnel and all my colleagues specially Mr. Muhammad Mohsin Riaz, who were of valuable assistance. At last, this effort could not have been completed if the sincere and earnest prayers and wishes of my whole family and friends were not there.

Dedication

To mom, dad (who has not lived to see this day) and brothers.

List of Abbreviations

DCT	Discrete Cosine Transform
DWT	Discrete Wavelet Transform
DFT	Discrete Fourier Transform
FIS	Fuzzy Inference System
GA	Genetic Algorithm
HVS	Human Visual System
JND	Just Noticeable Difference
JPEG	Joint Photographic Experts Group
NC	Normalized Correlation
PSNR	Peak Signal to Noise Ratio
PCA	Principal Component Analysis
PC	Principal Component
SVD	Singular Value Decomposition

Chapter 1

Introduction

In this chapter, a brief introduction about watermarking, its types, classification, application and the parameters used to measure the quality of watermarked image are discussed.

1.1 Introduction

The abrupt increase in the number of users of internet after the innovation of world wide web [1] has made internet a easy source of distribution of digital data (pictures, audio, video). Multiple copies of original data can be made easily with unnoticeable degradation and makes difficult to distinguish between original and copied data. This copied data can be distributed illegally without paying compensation to the original owner of data. Hence the content owners (authors, publishers, distributers, etc) are looking for a permanent solution that can assure the copyright protection. This creates problem of owner identification, authentication and copyright protection. There are two possible solutions : cryptography and watermarking [1].

Cryptography is the first and the most common method used for copyright protection. In cryptography the contents are encrypted before delivery, and the user who have purchased the contents are provided with decryption key. This decrypted data can be made available online. The lack/problem with cryptography is that once the purchased product is decrypted (using decryption key), it can be redistributed. Hence the encryption does not monitor the product once it is sold, how the user deals it after decryption. Watermarking has the possible solution to this problem [2], [3]. In watermarking some information (images, audio, video) can be embedded into the data in such a way that it is not perceptible to human eye. This hidden data can later be extracted to prove the ownership and ensures the appropriate payment to the actual owner [2], [4]. The generic diagram for watermark embedding and extraction process is shown in Figure 1.1

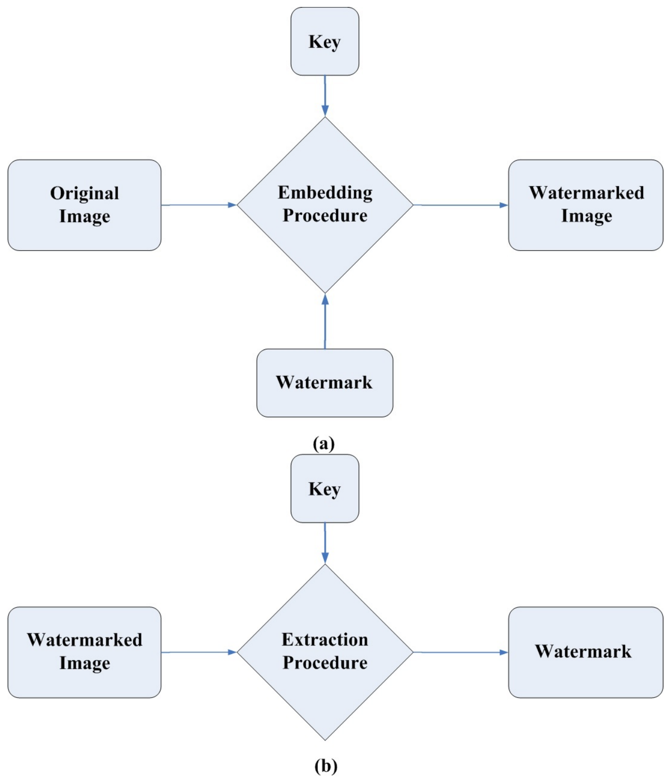

Figure 1.1: (a). Embedding Procedure (b). Extraction Procedure

1.2 Types of Watermarking

Watermarking can be divided into two major categories : visible and invisible [5]. In visible watermarking (simple watermarking technique) the watermark is embedded into a cover image in such a way that watermark is intentionally visible to a human observer [6]. The example includes a broadcasting channel where the logo is visible on top left corner as shown in Figure 1.2, or a stamp on paper. It is useful in case of immediate claim of ownership [5].

In invisible watermarking scheme, watermark (image, audio, video, text) is embedded

Figure 1.2: Visible Watermarking

into cover media (image, audio, video, text) in such a way that it is not perceptible by human sensors (eye, ear) but can be extracted with the help of computer program to claim the ownership [7].

1.3 Classification of Watermarking

Due to large number of variety of watermarking schemes, watermarking can be classified into numerous classes [5].

1.3.1 Robust, Fragile and Semi-Fragile Schemes

In robust watermarking schemes, the watermark needs to survive unintentional or intentional attacks until the original contents are destroyed [8]. It is useful in applications like ownership claim, fingerprinting, copy control, broadcast monitoring etc [8].

In fragile watermarking schemes, watermarks are destroyed completely in case of intentional or unintentional attacks [8], an opposite case of robust watermarking. It can be used for content authentication [9].

In semi-fragile watermarking schemes, the watermarks are fragile to certain alterations. It is used for content authentication and integrity verification [10].

1.3.2 Blind, Non-Blind, and Semi-Blind Schemes

In blind watermarking scheme, neither original image nor watermark (key) is needed for watermark extraction [11].

In non-blind watermarking schemes, original image is required at the time of extraction of watermark [12]. It is more secure than its counterparts as only those who have original image and key can extract the watermark.

In semi blind watermarking schemes, original image is not required at the time of extraction, but watermark (key) is required at the time of extraction [13].

1.3.3 Spatial and Frequency Domain Watermarking

Depending on domain watermarking can be classified into two categories: spatial and transform domain watermarking [4], [9], [11], [12], [14].

In spatial (time) domain watermarking schemes, the pixel values of the cover image are directly modified for watermark embedding [6], [12], [14]. Generally spatial domain watermarking scheme is less complex, less robust and less secure [3], [6], [12], [14], [15], [16].

In transform (frequency) domain the cover image is first transformed to other domain (using discrete cosine transform (DCT), discrete wavelet transform (DWT), discrete fourier transform (DFT) [3], [9], [15]) for watermark embedding [3]. The frequency domain watermarking schemes are relatively robust, secure and imperceptible [3], [14], [15].

1.4 Watermarking Application

Watermarking is useful for owner identification, fingerprinting, copy control, broadcast monitoring, authentication [1]. A owner identification mark is embedded into host media (image, audio, video), which later can be extracted to prove the ownership. The owner of content can embed unique watermarks in different host media. In case of illegal distribution the source can be traced. Illegitimate copying is another problem; that the owners of intellectual data are dealing with. The possible solution is to embed a watermark which when detected by the device, stop recording or copying of the original content. The watermark can be embedded into commercials to monitor, whether commercials are broadcasted or not for the time, they have paid for. In some cases (military, intelligence) the authenticity of the data is of high importance. In this case a watermark can be embedded into the host media, if watermark is detected, then the data is able to be trusted otherwise data has been altered (cannot be trusted).

1.5 Performance Evaluation

In order to be a useful watermark scheme, it should fulfil two contradictory requirements : robustness, and imperceptibility [2], [17]. Robustness (similarity between original and extracted watermark [4], [15]) is measured using normalized correlation coefficient (NC) and imperceptibility (quality of watermarked image [18] [19]) is measured using peak-signal-to-noise-ratio (PSNR). The watermarked image should be robust (can resist intentional or unintentional attacks like histogram equalization, rotation, Gaussian noise, scaling, cropping, Joint Photographic Experts Group (JPEG) compression, Y-shearing, X-shearing, median filtering, affine transformation, translation, salt and pepper, sharpening, blurring, average filtering) and imperceptible (i.e. there should be no visible difference between original and watermarked image).

Chapter 2

LITERATURE REVIEW

In this chapter the existing watermarking techniques for both gray and color images are reviewed to formulate the problem (the drawback with existing watermarking techniques are discussed). A summary of contributions is given. A brief introduction of the tools which are used in proposed schemes are discussed. These include DWT, singular value decomposition (SVD), principal component analysis (PCA).

2.1 Introduction

A number of image watermarking techniques appear in literature using just noticeable difference, spread spectrum approach, human visual system (HVS), genetic algorithm (GA), fuzzy inference system (FIS), integer to integer wavelet transform, DFT, DWT, interpolation based, DCT, SVD. Out of these tools DWT, SVD are famous for watermark embedding.

2.2 Review of Watermarking Schemes

In this section salient points about the state-of-the-art work of watermarking (in both gray and color images) is presented.

2.2.1 Schemes for Gray Images

Zhang et al proposed a scheme in which affine invariants are derived from Legendre moments and watermark is embedded on these invariants. This scheme is not robust against image cropping and histogram equalization [20].

Song et al proposed a scheme in which the predetermined bit-plane from lower frequency band is chosen for watermark embedding. This scheme does not perform well under median filtering, rotation and affine transformation attacks [21].

Lai et al proposed a scheme in which singular values of cover image are modified for watermark embedding, and GA is used to find the appropriate scaling factor.

Li et al proposed a scheme in which a cover image is decomposed into 8×8, and create a model by using fuzzy support vector machine, that can classify an image into high and weak texture regions. Watermark is scrambled using Arnold's transform. DCT is applied on each block of cover image, and is used the classification mode and to add watermark (with strong intensity if texture is found high and with weak intensity if texture is found weak). Reverse process is applied at the time of extraction [23].

Ganic et al proposed a scheme in which cover image is decomposed into its bands (LL, LH, HL and HH) using DWT. The singular values of watermark are embedded in the singular values of each band to get the watermarked image [7].

Using similar concept with some alterations Lai et al proposed a new scheme in which DWT is performed on cover image to get (LL, LH, HL and HH) bands. Watermark is divided into two parts and each part is added into the singular values of middle frequency band, to get watermarked image [14]. This scheme is robust and secure as compared to one in [7].

Dili et al proposed a scheme (similar to [14]) in which cover image is decomposed using one level Haar wavelet transform, and a random generated binary sequence is used to modify the singular values of LH and HL bands for watermark embedding. This scheme is useful against filter attacks [24].

Qui et al proposed a scheme in which HVS model of cover image is formed, divide the original and HVS model in 4×4 blocks. Watermark is introduced by modify each block of original image depending on random generated binary sequence and HVS model. This enhances imperceptibility [**?**].

2.2.2 Schemes for Color Images

Yin et al proposed a scheme in which green component (decomposed into LL, LH, HL and HH component using DWT) of the cover image is chosen for watermark embedding. The pseudo-random sequence of watermark (binary image of size 16*16) is embedded into LL band, whereas for other bands singular values (of watermark) are used for watermark embedding. The issue with this scheme is again imperceptibility, because channels (R, G and B) and not uncorrelated [2].

Rawat et al proposed a scheme in which YC_bC_r color space is chosen for watermark embedding. After performing DWT, singular values of watermark are calculated for all bands. DWT on each DCT block of cover image is performed and singular values of each band are calculated. The calculated singular values of watermark are added into the singular values of cover image to get the watermarked image [3]. In this scheme the original image is converted from RGB to YC_bC_r color space for un-correlating the color components. DWT and DCT both are used to increase the security level of watermarked image, one is sufficient, the use of two is making the scheme complicated.

Santhi et al proposed a scheme in which singular values of watermark are used to modify the singular values of DCT blocks of original image for watermark embedding. The cover image is converted to its color components (R, G and B). After applying DWT to each color space and low frequency band is divided into non-overlapping blocks (of size $4 * 4$) [4]. DCT is performed on each block. Singular values of watermark image are added into the singular values of DCT blocks to get the watermarked images. The issue with scheme is that it is very complicated and (R, G and B) channels are not uncorrelated, which affects the quality (imperceptibility) of watermarked image.

Thangavelu et al proposed a scheme in which singular values of watermark are added in singular values of all bands (LL, LH, HL and HH) in YUV color space for watermark embedding. This scheme is not good in terms of imperceptibility, if the scaling factor is increased (to increase the robustness) the quality of watermarked image will be degraded significantly [9], [18].

Dharwadkar et al proposed a scheme in which blue channel is decomposed using DWT. Singular values of watermark are used to modify the singular values of each band to obtain the watermarked image. There are two issues with this scheme, firstly the singular values of watermark (not the complete watermark) is embedded thus given scheme is not robust, secondly color channels are not uncorrelated before introducing the watermark which affects imperceptibility [15].

Baisa et al proposed a scheme in which a color image watermarking technique based on DWT and SVD is presented. R, G and B component of color image are converted to Y, I and Q respectively. In the YIQ color space Y component represent the intensity, I and Q component represents the color information. Then Q-component is chosen for embedding watermark. 3-level DWT of Q-component is performed to obtain (LL3, LH3, HL3, and HH3) bands. Adding watermark into the singular values of LL3 band of Q-component gives a new matrix. The singular values of this newly generated matrix are used to obtain modified LL3. Colored watermarked image is obtained to by taking inverse-DWT up to 3 levels. Imperceptibility is the drawback of this scheme [16].

Agarwal et al proposed a scheme in which eigen vectors of watermark are used to modify the eigen vector all color components (i.e. R, G and B), for watermark embedding. In this scheme, the watermark is directly embedded into original image without de-correlating the R, G and B channels, which degrades the quality of watermarked image, because the change in one channel will also affect on other channels as well [17].

Kapoor et al proposed a scheme in which HSV color space is chosen for watermark embedding. The H and V are decomposed into blocks and DCT of each block is performed. DWT is applied on each DCT block to get LL, LH, HL, and HH blocks. The non-overlapping blocks of watermark image are added in all bands (LL, LH, HL, and HH) to get watermarked image. This scheme is computationally complicated and does not give the satisfactory results [26].

2.3 Problem Formulation

The quality of watermarking scheme is primarily based on two conflicting requirements, robustness (measured using NC) and imperceptibility (measured using PSNR) [2], [17]. The existing schemes do not fulfill these two contradictory requirements at a time. If imperceptibility is improved, then robustness is decreased and vice versa. To achieve these (two) requirements in color image is a big task, because if out of three channels (R, G and B), the watermark embedded into one channel have impact on other channel because they are highly correlated [9], [16], [18] and this will affect on imperceptibility. So it is highly desirable to un-correlate these three (R, G and B) channels.

2.4 Contributions in This Thesis

Firstly, a color image is used as cover image whereas watermark is gray image (logo). PCA is used to un-correlate the three channels (R, G and B), to improve the imperceptibility. The second level DWT of first principal component is performed to achieve the security and watermark is embedded into the singular values of all bands (LL, LH, HL, and HH) to get the robustness. The imperceptibility of given scheme is measured using PSNR, and robustness is measured used NC after applying various attacks (histogram equalization, rotation, Gaussian noise, scaling, cropping, JPEG compression, Y-shearing, X-shearing, median filtering, affine transformation, translation, salt and pepper, sharpening, blurring, average filtering).

Secondly, a color watermark is embedded into the color cover image. The color watermark in this scheme is chosen to improve the robustness. PCA is used to un-correlate the three channels (R, G and B) of both cover image and of color watermark, to achieve the imperceptibility. The one level DWT of principal components of all the channels (R, G and B) of cover image are performed to achieve the security. The principal component of corresponding channel of color watermark is embedded into the singular values of corresponding channel's bands (LH and HL) to get the robustness. The imperceptibility of given scheme is measured using PSNR, and robustness is measured used NC after applying various attacks (histogram equalization, rotation, Gaussian noise, scaling, cropping, JPEG compression, Y-shearing, X-shearing, median filtering, affine transformation, translation, salt and pepper, sharpening, blurring, average filtering).

Thirdly (lastly) HVS (luminance masking and texture masking) was used to achieve the adaptive strength factor. As noise is less visible in dark areas as compared to bright areas so in dark areas watermark with large strength factor can be embedded, whereas in bright areas small strength factor will be used. Noise is less visible is textured areas as compared to smooth areas of an image, so watermark in textured areas are embedded with large strength factor whereas in smooth areas small strength factor will be used. So to achieve adaptive (dynamic) strength factor FIS is used. The imperceptibility of given scheme is measured using PSNR, and robustness is measured used NC after applying various attacks (histogram equalization, rotation, Gaussian noise, scaling, cropping, JPEG compression, Y-shearing, X-shearing, median filtering, affine transformation, translation, salt and pepper, sharpening, blurring, average filtering).

2.5 Discrete Wavelet Transform (DWT)

Image processing is made easy using wavelet transform (compressing, transmission, and analyzing of images [27]). Wavelet transform provide frequency and time information at the same time, whereas fourier transform provide only frequency information not temporal information [27]. An image can be decomposed up to any level using DWT. After performing one level DWT decomposition, four bands are formed, low frequency band (LL) and high frequency band (LH, HL, and HH) [4]. The LL band owns the coarse information, and (LH, HL and HH) band contain the finest level information [14]. The LL band can further be decomposed up to desired level. In Figure 2.1, three level DWT decomposition is shown: The LL band represents the image itself whereas (LH, HL, and

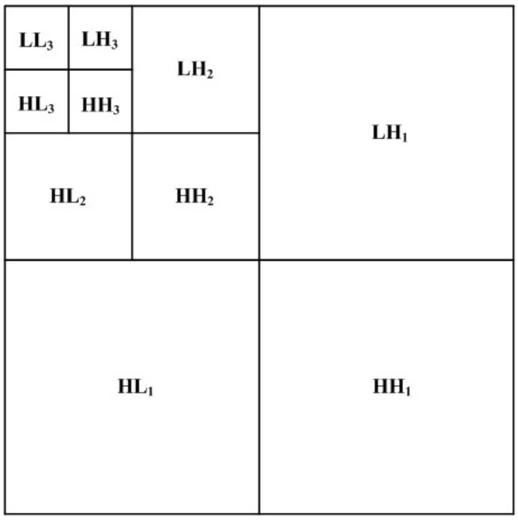

Figure 2.1: DWT decomposition upto 3 level

HH) bands represents the texture of an image [28], as shown in Fig. 2.2.

Figure 2.2: (a). Original Lena image (b). DWT decomposition

2.6 Singular Value Decomposition

From image processing point of view, an intensity image can be treated as non-negative real matrix [2], [14], [18], [19] . Any real (complex) matrix "A" can be decomposed into three matrices (i.e. $A = U\Sigma V^T$) [4], [7], [29], where U and V are orthogonal matrices [2], [4], [7], [14], [19] (i.e. $UU^T = I$ and $VV^T = I$, where I is an identity matrix) and Σ is diagonal matrix. This decomposition is called Singular Value Decomposition [2] [4], [7],

[19], [29]. Mathematically : $A = U\Sigma V^T$, where $U = [u_1, u_2, \ldots, u_m]$, $U = [v_1^T, v_2^T, \ldots, v_n^T]$ and

$$\Sigma = \begin{pmatrix} \lambda 1 & 0 & \ldots & 0 \\ 0 & \lambda_2 & \ldots & 0 \\ \vdots & \vdots & \ddots & \vdots \\ 0 & 0 & \ldots & \lambda_m \end{pmatrix}$$

where

$$\lambda_1 \geq \lambda_2 \geq \cdots \geq \lambda_m$$

In terms of U, λ and V, A can be written as:

$$A = \lambda_1 u_1 v_1^T + \lambda_2 u_2 v_2^T + \cdots + \lambda_m u_m v_m^T$$
$$A = \sum_{i=1}^{r} \lambda_i u_i v_i^T$$

where r is the rank of matrix A. The column of U are referred as "left singular vectors", column of V are referred as "right singular vectors" and diagonal of λ are "singular values" of A [4], [7], [14], [15], [18], [19], [29].

When a small change is made in image, it does not cause large variation in singular values [4], [9], [14], [15], [18]. Singular values own intrinsic properties of image (i.e. luminance information is contained in singular values, whereas geometric information is maintained by corresponding singular vectors) [2], [4], [14], [15], [19], [29]. The fixed size of matrix for SVD transformation is not required (square or rectangular matrix can be used) [29] Most of the information is maintained in highest singular values, so small singular values can be ignored without compromising the quality of image [2], [18].

2.7 Principal Component Analysis

PCA also called Karhunen-Loeve transform is used for dimension reduction [30] [31]. A new set of uncorrelated variables called principal components (PCs) from a set of highly correlated variables, are obtained using PCA [31]. Most of the variation are represented by first few PCs [31].

Following are steps to compute PCA

1. Obtain the original data Let a matrix X of dimension $M \times N$

$$X = \begin{pmatrix} x_{11} & x_{12} & \dots & x_{1N} \\ x_{21} & x_{22} & \dots & x_{2N} \\ \vdots & \vdots & \ddots & \vdots \\ x_{M1} & x_{M2} & \dots & x_{MN} \end{pmatrix}$$

2. Calculate mean

$$Mean = \frac{1}{MN} \sum_{i=1}^{M} \sum_{j=1}^{N} X(i,j)$$

3. Subtract mean from original data, the new data set will have zero mean

$$B = X - Mean$$

4. Calculate the covariance matrix

$$C = \frac{1}{MN} \sum_{i=1}^{M} \sum_{j=1}^{N} B(i,j) B^T(i,j)$$

   where T represents the transpose. The order of matrix C will be $M \times M$

5. Calculate the eigenvector and eigenvalues of covariance matrix C

$$
\begin{aligned}
C &= Q\Lambda Q^T \\
C &= \begin{pmatrix} q_{11} & q_{12} & \dots & q_{1N} \\ q_{21} & q_{22} & \dots & q_{2N} \\ \vdots & \vdots & \ddots & \vdots \\ q_{M1} & q_{M2} & \dots & q_{MN} \end{pmatrix} \begin{pmatrix} \Lambda_{11} & 0 & \dots & 0 \\ 0 & \Lambda_{22} & \dots & 0 \\ \vdots & \vdots & \ddots & \vdots \\ 0 & 0 & \dots & \Lambda_{MN} \end{pmatrix} \begin{pmatrix} q_{11} & q_{12} & \dots & q_{1N} \\ q_{21} & q_{22} & \dots & q_{2N} \\ \vdots & \vdots & \ddots & \vdots \\ q_{M1} & q_{M2} & \dots & q_{MN} \end{pmatrix}^T
\end{aligned}
$$

   where Q represents eigenvector matrix and Λ is eigenvalue matrix. Then eigenvectors and eigenvalues must be in descending order (i.e. $\Lambda_{11} > \Lambda_{22} > \Lambda_{33}$) and paired (i.e. K^{th} eigenvector is associated with K^{th} eigenvalue)

6. The projected components are formed as

$$Y = Q^T X$$

   The original matrix can be obtained as:

$$\hat{X} = QY$$

Chapter 3

Proposed Color Image Watermarking

Many watermarking schemes (for gray scale and color images) are available in literature. A watermarking scheme is said to be useful if it satisfies two contradictory requirements i.e. imperceptibility and robustness. The existing watermarking schemes are good either in terms of robustness or in terms of imperceptibility. These two requirements are not fulfilled at the same time specially for color images. In color images, the three channels R, G and B are highly correlated which should be uncorrelated before embedding watermark to improve the quality of watermarked image. In this thesis, these two requirements (i.e. imperceptibility and robustness) are met at the same time.

3.1 Color Image Watermarking Scheme 1

The three channels of color image (R, G and B) are uncorrelated before embedding watermark to improve the imperceptibility. The two level Haar DWT is performed for principal component (which contains most of the information), and watermark is embedded into the singular values of all bands (i.e. LL, LH, HL, and HH). The robustness is measured using NC and imperceptibility is measured using PSNR. This scheme is compared with existing schemes for various attacks (like histogram equalization, rotation, gaussian noise, scaling, cropping, JPEG compression, X-shearing, Y-shearing, median filtering, sharpening, salt and pepper, blurring, average filtering).

3.1.1 Watermark Embedding

Let the original color image I, is decomposed into its three components (R, G and B), where

$$R = \begin{pmatrix} r_{11} & r_{12} & \dots & r_{1N} \\ r_{21} & r_{22} & \dots & r_{2N} \\ \vdots & \vdots & \ddots & \vdots \\ r_{M1} & r_{M2} & \dots & r_{MN} \end{pmatrix}, G = \begin{pmatrix} g_{11} & g_{12} & \dots & g_{1N} \\ g_{21} & g_{22} & \dots & g_{2N} \\ \vdots & \vdots & \ddots & \vdots \\ g_{M1} & g_{M2} & \dots & g_{MN} \end{pmatrix}$$

$$B = \begin{pmatrix} b_{11} & b_{12} & \dots & b_{1N} \\ b_{21} & b_{22} & \dots & b_{2N} \\ \vdots & \vdots & \ddots & \vdots \\ b_{M1} & b_{M2} & \dots & b_{MN} \end{pmatrix}$$

M and N defines the size of the original image. Let a covariance matrix C be computed as

$$C = \frac{1}{MN}(AA^T) = Q\Lambda Q^{-1}$$

where

$$A = \begin{pmatrix} r_{11} \dots r_{1N} \, r_{21} \dots r_{2N} \dots r_{M1} \dots r_{MN} \\ g_{11} \dots g_{1N} \, g_{21} \dots g_{2N} \dots g_{M1} \dots g_{MN} \\ b_{11} \dots b_{1N} \, b_{21} \dots b_{2N} \dots b_{M1} \dots b_{MN} \end{pmatrix}$$

$$Q = \begin{pmatrix} q_{11} & q_{12} & q_{13} \\ q_{21} & q_{22} & q_{23} \\ q_{31} & q_{32} & q_{33} \end{pmatrix}, \qquad \Lambda = \begin{pmatrix} \lambda_{11} & 0 & 0 \\ 0 & \lambda_{22} & 0 \\ 0 & 0 & \lambda_{33} \end{pmatrix}$$

and $\lambda_{11} \geq \lambda_{22} \geq \lambda_{33}$

The principal components [31] of matrix C are written as

$$\begin{aligned} P &= \begin{pmatrix} P_r \\ P_g \\ P_b \end{pmatrix} = Q^T A \\ &= \begin{pmatrix} pr_{11} & \dots & pr_{1N} & pr_{21} & \dots & pr_{2N} & \dots & pr_{M1} & \dots & pr_{MN} \\ pg_{11} & \dots & pg_{1N} & pg_{21} & \dots & pg_{2N} & \dots & pg_{M1} & \dots & pg_{MN} \\ pb_{11} & \dots & pb_{1N} & pb_{21} & \dots & pb_{2N} & \dots & pb_{M1} & \dots & pb_{MN} \end{pmatrix} \end{aligned}$$

Since R, G and B components are highly correlated [9], [16], [18], the PCA [30] is used here to un-correlate these R, G and B channels. The first component of PCA (P_r) contains most of the image information [30].

Let matrix

$$Prn = \begin{pmatrix} pr_{11} & pr_{12} & \dots & pr_{1N} \\ pr_{21} & pr_{22} & \dots & pr_{2N} \\ \vdots & \vdots & \ddots & \vdots \\ pr_{M1} & pr_{M2} & \dots & pr_{MN} \end{pmatrix}$$

is decomposed into its sub-bands using DWT as following

$$\begin{aligned} \left(LL_1\, LH_1\, HL_1\, HH_1\right) &= DWT(P_{rn}) \\ \left(LL_2\, LH_2\, HL_2\, HH_2\right) &= DWT(LL_1) \end{aligned}$$

Since P_{rn} is composed of components from P_r and contains most of the color image information, therefore it is chosen for watermark embedding.

The use of DWT here is to improve the security level and robustness [15], [29]. The improvement in the security level and robustness is due to irregular distribution of watermark over the image during the inverse transform.

Let we decompose second level sub-bands as follows

$$\begin{aligned} LL_2 &= U_1 S_1 V_1^T \\ LH_2 &= U_2 S_2 V_2^T \\ HL_2 &= U_3 S_3 V_3^T \\ HH_2 &= U_4 S_4 V_4^T \end{aligned}$$

where S_1, S_2, S_3 and S_4 are diagonal matrices and contains singular values in descending order.

Small perturbation in image does not cause large variation in singular values [4], [9], [18]. Singular values own intrinsic properties of image (i.e. luminance information is contained in singular values, whereas geometric information is maintained by corresponding singular vectors) [2], [4], [18], [19], [29].

The watermark is introduced as following

$$\begin{aligned} S_1 + \alpha W &= U_{w1} S_{w1} V_{w1}^T \\ S_2 + \alpha(\frac{W}{2}) &= U_{w2} S_{w2} V_{w2}^T \\ S_3 + \alpha(\frac{W}{2}) &= U_{w3} S_{w3} V_{w3}^T \\ S_4 + \alpha W &= U_{w4} S_{w4} V_{w4}^T \end{aligned} \tag{3.1}$$

where S_{w1}, S_{w2}, S_{w3} and S_{w4} are diagonal matrices and contain singular values in descending order, W is the watermark and α defines the strength factor.

If the size of singular values matrix and watermark matrix mismatch in eq. 3.1, the watermark may be interpolated or decimated accordingly and reverse process applies for watermark extraction.

Let the modified sub-bands are as following

$$\begin{aligned} LL_w &= U_1 S_{w1} V_1^T \\ LH_w &= U_2 S_{w2} V_2^T \\ HL_w &= U_3 S_{w3} V_3^T \\ HH_w &= U_4 S_{w4} V_4^T \end{aligned}$$

The modified principal components are obtained as

$$\begin{aligned} P_w &= \begin{pmatrix} P_{rw} \\ P_g \\ P_b \end{pmatrix} \\ &= \begin{pmatrix} prw_{11} & \dots & prw_{1N} & prw_{21} & \dots & prw_{2N} & \dots & prw_{M1} & \dots & prw_{MN} \\ pg_{11} & \dots & pg_{1N} & pg_{21} & \dots & pg_{2N} & \dots & pg_{M1} & \dots & pg_{MN} \\ pb_{11} & \dots & pb_{1N} & pb_{21} & \dots & pb_{2N} & \dots & pb_{M1} & \dots & pb_{MN} \end{pmatrix} \end{aligned}$$

where

$$\begin{pmatrix} prw_{11} & prw_{12} & \dots & prw_{1N} \\ prw_{21} & prw_{22} & \dots & prw_{2N} \\ \vdots & \vdots & \ddots & \vdots \\ prw_{M1} & prw_{M2} & \dots & prw_{MN} \end{pmatrix} = IDWT(LL_w,\ LH_w,\ HL_w,\ HH_w)$$

The matrix A_w is obtained as

$$\begin{aligned} A_w &= QP_w \\ &= \begin{pmatrix} rw_{11} & \dots & rw_{1N} & rw_{21} & \dots & rw_{2N} & \dots & rw_{M1} & \dots & rw_{MN} \\ g_{11} & \dots & g_{1N} & g_{21} & \dots & g_{2N} & \dots & g_{M1} & \dots & g_{MN} \\ b_{11} & \dots & b_{1N} & b_{21} & \dots & b_{2N} & \dots & b_{M1} & \dots & b_{MN} \end{pmatrix} \end{aligned}$$

The watermarked image I_w is composed from (R_w, G, B) where

$$R_w = \begin{pmatrix} rw_{11} & rw_{12} & \dots & rw_{1N} \\ rw_{21} & rw_{22} & \dots & rw_{2N} \\ \vdots & \vdots & \ddots & \vdots \\ rw_{M1} & rw_{M2} & \dots & rw_{MN} \end{pmatrix}$$

3.1.2 Watermark Extraction

The received watermarked image $\hat{I_w}$ may be subject to perturbation (and attacks) on the watermarked image I_w.

Let $\hat{I}_w$ be decomposed into its components ($\hat{R}_w$, $\hat{G}$, $\hat{B}$), where

$$\hat{R_w} = \begin{pmatrix} \hat{r}w_{11} & \hat{r}w_{12} & \dots & \hat{r}w_{1N} \\ \hat{r}w_{21} & \hat{r}w_{22} & \dots & \hat{r}w_{2N} \\ \vdots & \vdots & \ddots & \vdots \\ \hat{r}w_{M1} & \hat{r}w_{M2} & \dots & \hat{r}w_{MN} \end{pmatrix} \hat{G} = \begin{pmatrix} \hat{g}_{11} & \hat{g}_{12} & \dots & \hat{g}_{1N} \\ \hat{g}_{21} & \hat{g}_{22} & \dots & \hat{g}_{2N} \\ \vdots & \vdots & \ddots & \vdots \\ \hat{g}_{M1} & \hat{g}_{M2} & \dots & g_{MN} \end{pmatrix}$$

$$\hat{B} = \begin{pmatrix} \hat{b}_{11} & \hat{b}_{12} & \dots & \hat{b}_{1N} \\ \hat{b}_{21} & \hat{b}_{22} & \dots & \hat{b}_{2N} \\ \vdots & \vdots & \ddots & \vdots \\ \hat{b}_{M1} & \hat{b}_{M2} & \dots & \hat{b}_{MN} \end{pmatrix}$$

Let a covariance matrix $\hat{C}$ be computed as

$$\hat{C} = \frac{1}{MN}(\hat{A}\hat{A}^T) = \hat{Q}\hat{\Lambda}\hat{Q}^{-1}$$

where

$$\hat{A} = \begin{pmatrix} \hat{r}w_{11} & \dots & \hat{r}w_{1N} & \hat{r}w_{21} & \dots & \hat{r}w_{2N} & \dots & \hat{r}w_{M1} & \dots & \hat{r}w_{MN} \\ \hat{g}_{11} & \dots & \hat{g}_{1N} & \hat{g}_{21} & \dots & \hat{g}_{2N} & \dots & \hat{g}_{M1} & \dots & \hat{g}_{MN} \\ \hat{b}_{11} & \dots & \hat{b}_{1N} & \hat{b}_{21} & \dots & \hat{b}_{2N} & \dots & \hat{b}_{M1} & \dots & \hat{b}_{MN} \end{pmatrix}$$

$$\hat{Q} = \begin{pmatrix} \hat{q}_{11} & \hat{q}_{12} & \hat{q}_{13} \\ \hat{q}_{21} & \hat{q}_{22} & \hat{q}_{23} \\ \hat{q}_{31} & \hat{q}_{32} & \hat{q}_{33} \end{pmatrix}, \qquad \hat{\Lambda} = \begin{pmatrix} \hat{\lambda}_{11} & 0 & 0 \\ 0 & \hat{\lambda}_{22} & 0 \\ 0 & 0 & \hat{\lambda}_{33} \end{pmatrix}$$

and $\hat{\lambda}_{11} \geq \hat{\lambda}_{22} \geq \hat{\lambda}_{33}$

The principal component of matrix $\hat{C}$ are written as

$$\begin{aligned} \hat{P}_w &= \begin{pmatrix} \hat{P}w_r \\ \hat{P}_g \\ \hat{P}_b \end{pmatrix} = \hat{Q}^T \hat{A} \\ &= \begin{pmatrix} \hat{p}rw_{11} & \dots & \hat{p}rw_{1N} & \hat{p}rw_{21} & \dots & \hat{p}rw_{2N} & \dots & \hat{p}rw_{M1} & \dots & \hat{p}rw_{MN} \\ \hat{p}g_{11} & \dots & \hat{p}g_{1N} & \hat{p}g_{21} & \dots & \hat{p}g_{2N} & \dots & \hat{p}g_{M1} & \dots & \hat{p}g_{MN} \\ \hat{p}b_{11} & \dots & \hat{p}b_{1N} & \hat{p}b_{21} & \dots & \hat{p}b_{2N} & \dots & \hat{p}b_{M1} & \dots & \hat{p}b_{MN} \end{pmatrix} \end{aligned}$$

Let the matrix

$$\hat{P}rnw = \begin{pmatrix} \hat{p}rw_{11} & \hat{p}rw_{12} & \dots & \hat{p}rw_{1N} \\ \hat{p}rw_{21} & \hat{p}rw_{22} & \dots & \hat{p}rw_{2N} \\ \vdots & \vdots & \ddots & \vdots \\ \hat{p}rw_{M1} & \hat{p}rw_{M2} & \dots & \hat{p}rw_{MN} \end{pmatrix}$$

is decomposed into its sub-bands using DWT as following

$$\begin{aligned} \begin{pmatrix} \hat{LL}_1 & \hat{LH}_1 & \hat{HL}_1 & \hat{HH}_1 \end{pmatrix} &= DWT(\hat{P}_{rnw}) \\ \begin{pmatrix} \hat{LL}_2 & \hat{LH}_2 & \hat{HL}_2 & \hat{HH}_2 \end{pmatrix} &= DWT(\hat{LL}_1) \end{aligned}$$

Let we decompose second level sub-bands as follows

$$
\begin{aligned}
\hat{LL}_2 &= \hat{U}_1 \hat{S}_1 \hat{V}_1^T, \\
\hat{LH}_2 &= \hat{U}_2 \hat{S}_2 \hat{V}_2^T, \\
\hat{HL}_2 &= \hat{U}_3 \hat{S}_3 \hat{V}_3^T, \\
\hat{HH}_2 &= \hat{U}_4 \hat{S}_4 \hat{V}_4^T,
\end{aligned}
$$

Watermarks extracted are

$$
\begin{aligned}
W_{LL} &= \frac{U_{w1} \hat{S}_1 V_{w1}^T - S_1}{\alpha} \\
W_{LH\&HL} &= \frac{U_{w2} \hat{S}_2 V_{w2}^T - S_2}{\alpha} + \frac{U_{w3} \hat{S}_3 V_{w3}^T - S_3}{\alpha} \\
W_{HH} &= \frac{U_{w4} \hat{S}_4 V_{w4}^T - S_4}{\alpha}
\end{aligned}
$$

There are three watermarks W_{LL} extracted from LL band, W_{HH} from HH band and $W_{LH\&HL}$ extracted from LH and HL band. The watermark $\hat{W}$ with highest NC is the extracted watermark (out of W_{LL}, W_{HH}, and $W_{LH\&HL}$).
The proposed schemes satisfies both requirements imperceptibility and robustness. This scheme is robust against many attacks specially geometric attacks (rotation, cropping, scaling, affine transformation, shearing, etc) which are difficult to deal with.

3.2 Color Image Watermarking Scheme 2

The robustness of watermarking scheme is increased if the amount of embedding information is increased, but this will decrease the imperceptibility. The more information we embed into the color image, the chances to remove the watermark with intentional or unintentional attacks will be less. In this scheme a complete color watermark is embedded to color cover image to improve the robustness and security level. On the other side, the imperceptibility is maintained by un-correlating the three channels (R, G and B) of both watermark and cover image using PCA. The one level Haar wavelet transform is performed on each principal components of color cover image. The PCs of watermark are embedding into the singular values of (LH and HL) bands of corresponding PCs of color cover image. The quality of the watermarked image (i.e. imperceptibility) is measured using PSNR, and robustness is measured using NC.

3.2.1 Watermark Embedding

Let the color watermark W, is decomposed into its three channels (W_r, W_g, and W_b), where

$$W_r = \begin{pmatrix} wr_{11} & wr_{12} & \dots & wr_{1n} \\ wr_{21} & wr_{22} & \dots & wr_{2n} \\ \vdots & \vdots & \ddots & \vdots \\ wr_{m1} & wr_{m2} & \dots & wr_{mn} \end{pmatrix}, W_g = \begin{pmatrix} wg_{11} & wg_{12} & \dots & wg_{1n} \\ wg_{21} & wg_{22} & \dots & wg_{2n} \\ \vdots & \vdots & \ddots & \vdots \\ wg_{m1} & wg_{m2} & \dots & wg_{mn} \end{pmatrix},$$

$$W_b = \begin{pmatrix} wb_{11} & wb_{12} & \dots & wb_{1n} \\ wb_{21} & wb_{22} & \dots & wb_{2n} \\ \vdots & \vdots & \ddots & \vdots \\ wb_{m1} & wb_{m2} & \dots & wb_{mn} \end{pmatrix}$$

m and n defines the size of the watermark.

Let a covariance matrix Cw is computed as

$$Cw = \frac{1}{mn}(W_1 W_1^T) = Q_w \Lambda_w Q_w^{-1}$$

where

$$W_1 = \begin{pmatrix} wr_{11} & \dots & wr_{1n} & wr_{21} & \dots & wr_{2n} & \dots & wr_{m1} & \dots & wr_{mn} \\ wg_{11} & \dots & wg_{1n} & wg_{21} & \dots & wg_{2n} & \dots & wg_{m1} & \dots & wg_{mn} \\ wb_{11} & \dots & wb_{1n} & wb_{21} & \dots & wb_{2n} & \dots & wb_{m1} & \dots & wb_{mn} \end{pmatrix},$$

$$Q_w = \begin{pmatrix} wq_{11} & wq_{12} & wq_{13} \\ wq_{21} & wq_{22} & wq_{23} \\ wq_{31} & wq_{32} & wq_{33} \end{pmatrix}, \qquad \Lambda w = \begin{pmatrix} \lambda w_1 & 0 & 0 \\ 0 & \lambda w_2 & 0 \\ 0 & 0 & \lambda w_3 \end{pmatrix}$$

and $\lambda w_1 \geq \lambda w_2 \geq \lambda w_3$

The principal components [16] of matrix Cw are written as

$$Pw = \begin{pmatrix} Pw_r \\ Pw_g \\ Pw_b \end{pmatrix} = Q_w^T W_1 \tag{3.2}$$

where

$$\begin{aligned} Pw_r &= \begin{pmatrix} pwr_{11} & \dots & pwr_{1n} & pwr_{21} & \dots & pwr_{2n} & \dots & pwr_{m1} & \dots & pwr_{mn} \end{pmatrix} \\ Pw_g &= \begin{pmatrix} pwg_{11} & \dots & pwg_{1n} & pwg_{21} & \dots & pwg_{2n} & \dots & pwg_{m1} & \dots & pwg_{mn} \end{pmatrix} \\ Pw_b &= \begin{pmatrix} pwb_{11} & \dots & pwb_{1n} & pwb_{21} & \dots & pwb_{2n} & \dots & pwb_{m1} & \dots & pwb_{mn} \end{pmatrix} \end{aligned}$$

Let the original color image I, is decomposed into its three components (I_r, I_g and

I_b), where

$$I_r = \begin{pmatrix} r_{11} & r_{12} & \dots & r_{1N} \\ r_{21} & r_{22} & \dots & r_{2N} \\ \vdots & \vdots & \ddots & \vdots \\ r_{M1} & r_{M2} & \dots & r_{MN} \end{pmatrix}, I_g = \begin{pmatrix} g_{11} & g_{12} & \dots & g_{1N} \\ g_{21} & g_{22} & \dots & g_{2N} \\ \vdots & \vdots & \ddots & \vdots \\ g_{M1} & g_{M2} & \dots & g_{MN} \end{pmatrix},$$

$$I_b = \begin{pmatrix} b_{11} & b_{12} & \dots & b_{1N} \\ b_{21} & b_{22} & \dots & b_{2N} \\ \vdots & \vdots & \ddots & \vdots \\ b_{M1} & b_{M2} & \dots & b_{MN} \end{pmatrix}$$

M and N defines the size of the original image.

Let a covariance matrix C_I be computed as

$$C_I = \frac{1}{MN}(I_1 I_1^T) = Q_I \Lambda_I Q_I^{-1}$$

where

$$I_1 = \begin{pmatrix} r_{11} & \dots & r_{1N} & r_{21} & \dots & r_{2N} & \dots & r_{M1} & \dots & r_{MN} \\ g_{11} & \dots & g_{1N} & g_{21} & \dots & g_{2N} & \dots & g_{M1} & \dots & g_{MN} \\ b_{11} & \dots & b_{1N} & b_{21} & \dots & b_{2N} & \dots & b_{M1} & \dots & b_{MN} \end{pmatrix},$$

$$Q_I = \begin{pmatrix} q_{11} & q_{12} & q_{13} \\ q_{21} & q_{22} & q_{23} \\ q_{31} & q_{32} & q_{33} \end{pmatrix}, \qquad \Lambda_I = \begin{pmatrix} \lambda_1 & 0 & 0 \\ 0 & \lambda_2 & 0 \\ 0 & 0 & \lambda_3 \end{pmatrix}$$

and $\lambda_1 \geq \lambda_2 \geq \lambda_3$

The principal components [16] of matrix C_I are written as

$$P_I = \begin{pmatrix} P_{Ir} \\ P_{Ig} \\ P_{Ib} \end{pmatrix} = Q_I^T I_1$$

$$\begin{aligned}
P_{Ir} &= \begin{pmatrix} pr_{11} & \dots & pr_{1N} & pr_{21} & \dots & pr_{2N} & \dots & pr_{M1} & \dots & pr_{MN} \end{pmatrix} \\
P_{Ig} &= \begin{pmatrix} pg_{11} & \dots & pg_{1N} & pg_{21} & \dots & pg_{2N} & \dots & pg_{M1} & \dots & pg_{MN} \end{pmatrix} \\
P_{Ib} &= \begin{pmatrix} pb_{11} & \dots & pb_{1N} & pb_{21} & \dots & pb_{2N} & \dots & pb_{M1} & \dots & pb_{MN} \end{pmatrix}
\end{aligned}$$

Let the matrices

$$Prn = \begin{pmatrix} pr_{11} & pr_{12} & \dots & pr_{1N} \\ pr_{21} & pr_{22} & \dots & pr_{2N} \\ \vdots & \vdots & \ddots & \vdots \\ pr_{M1} & pr_{M2} & \dots & pr_{MN} \end{pmatrix}, Pgn = \begin{pmatrix} pg_{11} & pg_{12} & \dots & pg_{1N} \\ pg_{21} & pg_{22} & \dots & pg_{2N} \\ \vdots & \vdots & \ddots & \vdots \\ pg_{M1} & pg_{M2} & \dots & pg_{MN} \end{pmatrix},$$

$$Pbn = \begin{pmatrix} pb_{11} & pb_{12} & \dots & pb_{1N} \\ pb_{21} & pb_{22} & \dots & pb_{2N} \\ \vdots & \vdots & \ddots & \vdots \\ pb_{M1} & pb_{M2} & \dots & pb_{MN} \end{pmatrix}$$

are decomposed into their sub-bands using DWT as following

$$\begin{aligned}
\begin{pmatrix} LL_r & LH_r & HL_r & HH_r \end{pmatrix} &= DWT(P_{rn}) \\
\begin{pmatrix} LL_g & LH_g & HL_g & HH_g \end{pmatrix} &= DWT(P_{gn}) \\
\begin{pmatrix} LL_b & LH_b & HL_b & HH_b \end{pmatrix} &= DWT(P_{bn})
\end{aligned}$$

Let we decompose sub-bands of each channel as follows

$$\begin{aligned}
LH_r &= Ur_1 Sr_1 Vr_1^T \\
HL_r &= Ur_2 Sr_2 Vr_2^T \\
LH_g &= Ug_1 Sg_1 Vg_1^T \\
HL_g &= Ug_2 Sg_2 Vg_2^T \\
LH_b &= Ub_1 Sb_1 Vb_1^T \\
HL_b &= Ub_2 Sb_2 Vb_2^T
\end{aligned}$$

where Sr_1, Sr_2, Sg_1, Sg_2 Sb_1, and Sb_2 are diagonal matrices and contains singular values in descending order.

The watermark is introduced as following

$$
\begin{aligned}
Sr_1 + \alpha(\frac{Pw_{1r}}{2}) &= Ur_{w1}Sr_{w1}Vr_{w1}^T \\
Sr_2 + \alpha(\frac{Pw_{1r}}{2}) &= Ur_{w2}Sr_{w2}Vr_{w2}^T \\
Sg_1 + \alpha(\frac{Pw_{1g}}{2}) &= Ug_{w1}Sg_{w1}Vg_{w1}^T \\
Sg_2 + \alpha(\frac{Pw_{1g}}{2}) &= Ug_{w2}Sg_{w2}Vg_{w2}^T \\
Sb_1 + \alpha(\frac{Pw_{1b}}{2}) &= Ub_{w1}Sb_{w1}Vb_{w1}^T \\
Sb_2 + \alpha(\frac{Pw_{1b}}{2}) &= Ub_{w2}Sb_{w2}Vb_{w2}^T
\end{aligned}
$$

where

$$
Pw_{1r} = \begin{pmatrix} pwr_{11} & pwr_{12} & \dots & pwr_{1n} \\ pwr_{21} & pwr_{22} & \dots & pwr_{2n} \\ \vdots & \vdots & \ddots & \vdots \\ pwr_{m1} & pwr_{m2} & \dots & pwr_{mn} \end{pmatrix},
$$

$$
Pw_{1g} = \begin{pmatrix} pwg_{11} & pwg_{12} & \dots & pwg_{1n} \\ pwg_{21} & pwg_{22} & \dots & pwg_{2n} \\ \vdots & \vdots & \ddots & \vdots \\ pwg_{m1} & pwg_{m2} & \dots & pwg_{mn} \end{pmatrix},
$$

$$
Pw_{1b} = \begin{pmatrix} pwb_{11} & pwb_{12} & \dots & pwb_{1n} \\ pwb_{21} & pwb_{22} & \dots & pwb_{2n} \\ \vdots & \vdots & \ddots & \vdots \\ pwb_{m1} & pwb_{m2} & \dots & pwb_{mn} \end{pmatrix}
$$

where Sr_{w1}, Sr_{w2}, Sg_{w1}, Sg_{w2}, Sb_{w1} and Sb_{w2} are diagonal singular values matrices and contain singular values in descending order. Pw_{1r}, Pw_{1g} and Pw_{1b} are the independent red, green and blue components of the watermark obtained from first, second and third row of eq. 3.2 respectively and α defines the strength factor.

Let the modified sub-bands are as following

$$
\begin{aligned}
LHr_w &= Ur_1 Sr_{w1} Vr_1^T \\
HLr_w &= Ur_2 Sr_{w2} Vr_2^T \\
LHg_w &= Ug_1 Sg_{w1} Vg_1^T \\
HLg_w &= Ug_2 Sg_{w2} Vg_2^T \\
LHr_w &= Ur_1 Sr_{w1} Vr_1^T \\
HLr_w &= Ur_2 Sr_{w2} Vr_2^T
\end{aligned}
$$

The modified principal components are obtained as

$$
\begin{aligned}
P_w &= \begin{pmatrix} Pr_w \\ Pg_w \\ Pb_w \end{pmatrix} \\
&= \begin{pmatrix} prw_{11} \dots prw_{1N}\, prw_{21} \dots prw_{2N} \dots prw_{M1} \dots prw_{MN} \\ pgw_{11} \dots pgw_{1N}\, pgw_{21} \dots pgw_{2N} \dots pgw_{M1} \dots pgw_{MN} \\ pbw_{11} \dots pbw_{1N}\, pbw_{21} \dots pbw_{2N} \dots pbw_{M1} \dots pbw_{MN} \end{pmatrix}
\end{aligned}
$$

where

$$
\begin{pmatrix} prw_{11} & prw_{12} & \dots & prw_{1N} \\ prw_{21} & prw_{22} & \dots & prw_{2N} \\ \vdots & \vdots & \ddots & \vdots \\ prw_{M1} & prw_{M2} & \dots & prw_{MN} \end{pmatrix} = IDWT(LL,\ LHr_w,\ HLr_w,\ HH)
$$

$$\begin{pmatrix} pgw_{11} & pgw_{12} & \dots & pgw_{1N} \\ pgw_{21} & pgw_{22} & \dots & pgw_{2N} \\ \vdots & \vdots & \ddots & \vdots \\ pgw_{M1} & pgw_{M2} & \dots & pgw_{MN} \end{pmatrix} = IDWT(LL,\ LHg_w,\ HLg_w,\ HH)$$

$$\begin{pmatrix} pbw_{11} & pbw_{12} & \dots & pbw_{1N} \\ pbw_{21} & pbw_{22} & \dots & pbw_{2N} \\ \vdots & \vdots & \ddots & \vdots \\ pbw_{M1} & pbw_{M2} & \dots & pbw_{MN} \end{pmatrix} = IDWT(LL,\ LHb_w,\ HLb_w,\ HH)$$

The matrix I_w is obtained as

$$\begin{aligned} I_w &= Q_I P_w \\ &= \begin{pmatrix} rw_{11} & \dots & rw_{1N} & rw_{21} & \dots & rw_{2N} & \dots & rw_{M1} & \dots & rw_{MN} \\ gw_{11} & \dots & gw_{1N} & gw_{21} & \dots & gw_{2N} & \dots & gw_{M1} & \dots & gw_{MN} \\ bw_{11} & \dots & bw_{1N} & bw_{21} & \dots & bw_{2N} & \dots & bw_{M1} & \dots & bw_{MN} \end{pmatrix} \end{aligned}$$

The watermarked image I_w is composed from (R_w, G_w, B_w) where

$$R_w = \begin{pmatrix} rw_{11} & rw_{12} & \dots & rw_{1N} \\ rw_{21} & rw_{22} & \dots & rw_{2N} \\ \vdots & \vdots & \ddots & \vdots \\ rw_{M1} & rw_{M2} & \dots & rw_{MN} \end{pmatrix}, \quad G_w = \begin{pmatrix} gw_{11} & gw_{12} & \dots & gw_{1N} \\ gw_{21} & gw_{22} & \dots & gw_{2N} \\ \vdots & \vdots & \ddots & \vdots \\ gw_{M1} & gw_{M2} & \dots & gw_{MN} \end{pmatrix},$$

$$B_w = \begin{pmatrix} bw_{11} & bw_{12} & \dots & bw_{1N} \\ bw_{21} & bw_{22} & \dots & bw_{2N} \\ \vdots & \vdots & \ddots & \vdots \\ bw_{M1} & bw_{M2} & \dots & bw_{MN} \end{pmatrix}$$

3.2.2 Watermark Extraction

The received watermarked image $\hat{I_w}$ may be subject to perturbation (and attacks) on the watermarked image I_w. Let $\hat{I}_w$ be decomposed into its components ($\hat{R}_w$, $\hat{G}_w$, $\hat{B}_w$), where

$$\hat{R_w} = \begin{pmatrix} \hat{r}w_{11} & \hat{r}w_{12} & \dots & \hat{r}w_{1N} \\ \hat{r}w_{21} & \hat{r}w_{22} & \dots & \hat{r}w_{2N} \\ \vdots & \vdots & \ddots & \vdots \\ \hat{r}w_{M1} & \hat{r}w_{M2} & \dots & \hat{r}w_{MN} \end{pmatrix}, \quad \hat{G_w} = \begin{pmatrix} \hat{g}w_{11} & \hat{g}w_{12} & \dots & \hat{g}w_{1N} \\ \hat{g}w_{21} & \hat{g}w_{22} & \dots & \hat{g}w_{2N} \\ \vdots & \vdots & \ddots & \vdots \\ \hat{g}w_{M1} & \hat{g}w_{M2} & \dots & \hat{g}w_{MN} \end{pmatrix},$$

$$\hat{B_w} = \begin{pmatrix} \hat{b}w_{11} & \hat{b}w_{12} & \dots & \hat{b}w_{1N} \\ \hat{b}w_{21} & \hat{b}w_{22} & \dots & \hat{b}w_{2N} \\ \vdots & \vdots & \ddots & \vdots \\ \hat{b}w_{M1} & \hat{b}w_{M2} & \dots & \hat{b}w_{MN} \end{pmatrix}$$

Let a covariance matrix $\hat{C}_I$ be computed as

$$\hat{C}_I = \frac{1}{MN}(\hat{I}_1\hat{I}_1^T) = \hat{Q}_I\hat{\Lambda}_I\hat{Q}_I^{-1}$$

where

$$\hat{I}_1 = \begin{pmatrix} \hat{r}w_{11} & \dots & \hat{r}w_{1N} & \hat{r}w_{21} & \dots & \hat{r}w_{2N} & \dots & \hat{r}w_{M1} & \dots & \hat{r}w_{MN} \\ \hat{g}w_{11} & \dots & \hat{g}w_{1N} & \hat{g}w_{21} & \dots & \hat{g}w_{2N} & \dots & \hat{g}w_{M1} & \dots & \hat{g}w_{MN} \\ \hat{b}w_{11} & \dots & \hat{b}w_{1N} & \hat{b}w_{21} & \dots & \hat{b}w_{2N} & \dots & \hat{b}w_{M1} & \dots & \hat{b}w_{MN} \end{pmatrix},$$

$$\hat{Q}_I = \begin{pmatrix} \hat{q}_{11} & \hat{q}_{12} & \hat{q}_{13} \\ \hat{q}_{21} & \hat{q}_{22} & \hat{q}_{23} \\ \hat{q}_{31} & \hat{q}_{32} & \hat{q}_{33} \end{pmatrix}, \qquad \hat{\Lambda}_I = \begin{pmatrix} \hat{\lambda}_1 & 0 & 0 \\ 0 & \hat{\lambda}_2 & 0 \\ 0 & 0 & \hat{\lambda}_3 \end{pmatrix}$$

and $\hat{\lambda}_1 \geq \hat{\lambda}_2 \geq \hat{\lambda}_3$

The principal component of matrix $\hat{C}_I$ are written as

$$\hat{P}_w = \begin{pmatrix} \hat{P}w_r \\ \hat{P}w_g \\ \hat{P}w_b \end{pmatrix} = \hat{Q}_I^T \hat{I}_1$$

where

$$\begin{aligned}
\hat{P}w_r &= \begin{pmatrix} \hat{p}rw_{11} & \dots & \hat{p}rw_{1N} & \hat{p}rw_{21} & \dots & \hat{p}rw_{2N} & \dots & \hat{p}rw_{M1} & \dots & \hat{p}rw_{MN} \end{pmatrix} \\
\hat{P}w_g &= \begin{pmatrix} \hat{p}gw_{11} & \dots & \hat{p}gw_{1N} & \hat{p}gw_{21} & \dots & \hat{p}gw_{2N} & \dots & \hat{p}gw_{M1} & \dots & \hat{p}gw_{MN} \end{pmatrix} \\
\hat{P}w_b &= \begin{pmatrix} \hat{p}bw_{11} & \dots & \hat{p}bw_{1N} & \hat{p}bw_{21} & \dots & \hat{p}bw_{2N} & \dots & \hat{p}bw_{M1} & \dots & \hat{p}bw_{MN} \end{pmatrix}
\end{aligned}$$

Let the matrices

$$\begin{aligned}
\hat{P}rnw &= \begin{pmatrix} \hat{p}rw_{11} & \hat{p}rw_{12} & \dots & \hat{p}rw_{1N} \\ \hat{p}rw_{21} & \hat{p}rw_{22} & \dots & \hat{p}rw_{2N} \\ \vdots & \vdots & \ddots & \vdots \\ \hat{p}rw_{M1} & \hat{p}rw_{M2} & \dots & \hat{p}rw_{MN} \end{pmatrix}, \\
\hat{P}gnw &= \begin{pmatrix} \hat{p}gw_{11} & \hat{p}gw_{12} & \dots & \hat{p}gw_{1N} \\ \hat{p}gw_{21} & \hat{p}gw_{22} & \dots & \hat{p}gw_{2N} \\ \vdots & \vdots & \ddots & \vdots \\ \hat{p}gw_{M1} & \hat{p}gw_{M2} & \dots & \hat{p}gw_{MN} \end{pmatrix}, \\
\hat{P}bnw &= \begin{pmatrix} \hat{p}bw_{11} & \hat{p}bw_{12} & \dots & \hat{p}bw_{1N} \\ \hat{p}bw_{21} & \hat{p}bw_{22} & \dots & \hat{p}bw_{2N} \\ \vdots & \vdots & \ddots & \vdots \\ \hat{p}bw_{M1} & \hat{p}bw_{M2} & \dots & \hat{p}bw_{MN} \end{pmatrix}
\end{aligned}$$

are decomposed into their sub-bands using DWT as following

$$\begin{aligned}
\begin{pmatrix} \hat{LL}_r & \hat{LH}_r & \hat{HL}_r & \hat{HH}_r \end{pmatrix} &= DWT(\hat{P}_{rnw}) \\
\begin{pmatrix} \hat{LL}_g & \hat{LH}_g & \hat{HL}_g & \hat{HH}_g \end{pmatrix} &= DWT(\hat{P}_{gnw}) \\
\begin{pmatrix} \hat{LL}_b & \hat{LH}_b & \hat{HL}_b & \hat{HH}_b \end{pmatrix} &= DWT(\hat{P}_{bnw})
\end{aligned}$$

Sub-bands of each channel as decomposed as follows

$$\begin{aligned}
\hat{LH}_r &= \hat{U}r_1\hat{S}r_1\hat{V}r_1^T, \\
\hat{HL}_r &= \hat{U}r_2\hat{S}r_2\hat{V}r_2^T, \\
\hat{LH}_g &= \hat{U}g_1\hat{S}g_1\hat{V}g_1^T, \\
\hat{HL}_g &= \hat{U}g_2\hat{S}g_2\hat{V}g_2^T, \\
\hat{LH}_b &= \hat{U}b_1\hat{S}b_1\hat{V}b_1^T, \\
\hat{HL}_b &= \hat{U}b_2\hat{S}b_2\hat{V}b_2^T,
\end{aligned}$$

The projected values of watermark are obtained as follows

$$\begin{aligned}
\hat{P}w_r &= \frac{Ur_{w1}\hat{S}r_1Vr_{w1}^T - Sr_1}{\alpha} + \frac{Ur_{w2}\hat{S}r_2Vr_{w2}^T - Sr_2}{\alpha} \\
\hat{P}w_g &= \frac{Ug_{w1}\hat{S}g_1Vg_{w1}^T - Sg_1}{\alpha} + \frac{Ug_{w2}\hat{S}g_2Vg_{w2}^T - Sg_2}{\alpha} \\
\hat{P}w_b &= \frac{Ub_{w1}\hat{S}b_1Vb_{w1}^T - Sb_1}{\alpha} + \frac{Ub_{w2}\hat{S}b_2Vb_{w2}^T - Sb_2}{\alpha}
\end{aligned}$$

where

$$\hat{P}w_r=\begin{pmatrix} \hat{p}wr_{11} & \hat{p}wr_{12} & \ldots & \hat{p}wr_{1n} \\ \hat{p}wr_{21} & \hat{p}wr_{22} & \ldots & \hat{p}wr_{2n} \\ \vdots & \vdots & \ddots & \vdots \\ \hat{p}wr_{m1} & \hat{p}wr_{m2} & \ldots & \hat{p}wr_{mn} \end{pmatrix},$$

$$\hat{P}w_g=\begin{pmatrix} \hat{p}wg_{11} & \hat{p}wg_{12} & \ldots & \hat{p}wg_{1n} \\ \hat{p}wg_{21} & \hat{p}wg_{22} & \ldots & \hat{p}wg_{2n} \\ \vdots & \vdots & \ddots & \vdots \\ \hat{p}wg_{m1} & \hat{p}wg_{m2} & \ldots & \hat{p}wg_{mn} \end{pmatrix},$$

$$\hat{P}w_b = \begin{pmatrix} \hat{p}wb_{11} & \hat{p}wb_{12} & \ldots & \hat{p}wb_{1n} \\ \hat{p}wb_{21} & \hat{p}wb_{22} & \ldots & \hat{p}wb_{2n} \\ \vdots & \vdots & \ddots & \vdots \\ \hat{p}wb_{m1} & \hat{p}wb_{m2} & \ldots & \hat{p}wb_{mn} \end{pmatrix}$$

The watermark is recovered as follows

$$\hat{W}_1 = Q_w\hat{P}w = \begin{pmatrix} \hat{w}r_{11} & \ldots & \hat{w}r_{1n} & \hat{w}r_{21} & \ldots & \hat{w}r_{2n} & \ldots \hat{w}r_{m1} & \ldots & \hat{w}r_{mn} \\ \hat{w}g_{11} & \ldots & \hat{w}g_{1n} & \hat{w}g_{21} & \ldots & \hat{w}g_{2n} & \ldots \hat{w}g_{m1} & \ldots & \hat{w}g_{mn} \\ \hat{w}b_{11} & \ldots & \hat{w}b_{1n} & \hat{w}b_{21} & \ldots & \hat{w}b_{2n} & \ldots \hat{w}b_{m1} & \ldots & \hat{w}b_{mn} \end{pmatrix}$$

where

$$\hat{P}w = \begin{pmatrix} \hat{p}wr_{11} & \ldots & \hat{p}wr_{1n} & \hat{p}wr_{21} & \ldots & \hat{p}wr_{2n} & \ldots & \hat{p}wr_{m1} & \ldots & \hat{p}wr_{mn} \\ \hat{p}wg_{11} & \ldots & \hat{p}wg_{1n} & \hat{p}wg_{21} & \ldots & \hat{p}wg_{2n} & \ldots & \hat{p}wg_{m1} & \ldots & \hat{p}wg_{mn} \\ \hat{p}wb_{11} & \ldots & \hat{p}wb_{1n} & \hat{p}wb_{21} & \ldots & \hat{p}wb_{2n} & \ldots & \hat{p}wb_{m1} & \ldots & \hat{p}wb_{mn} \end{pmatrix}$$

The recovered watermark $\hat{W}$ is obtained from three channels ($\hat{W}_r$, $\hat{W}_g$, and $\hat{W}_b$), where

$$\hat{W}_r = \begin{pmatrix} \hat{w}r_{11} & \hat{w}r_{12} & \dots & \hat{w}r_{1n} \\ \hat{w}r_{21} & \hat{w}r_{22} & \dots & \hat{w}r_{2n} \\ \vdots & \vdots & \ddots & \vdots \\ \hat{w}r_{m1} & \hat{w}r_{m2} & \dots & \hat{w}r_{mn} \end{pmatrix}, \quad \hat{W}_g = \begin{pmatrix} \hat{w}g_{11} & \hat{w}g_{12} & \dots & \hat{w}g_{1n} \\ \hat{w}g_{21} & \hat{w}g_{22} & \dots & \hat{w}g_{2n} \\ \vdots & \vdots & \ddots & \vdots \\ \hat{w}g_{m1} & \hat{w}g_{m2} & \dots & \hat{w}g_{mn} \end{pmatrix},$$

$$\hat{W}_b = \begin{pmatrix} \hat{w}b_{11} & \hat{w}b_{12} & \dots & \hat{w}b_{1n} \\ \hat{w}b_{21} & \hat{w}b_{22} & \dots & \hat{w}b_{2n} \\ \vdots & \vdots & \ddots & \vdots \\ \hat{w}b_{m1} & \hat{w}b_{m2} & \dots & \hat{w}b_{mn} \end{pmatrix}$$

This schemes provides robustness, imperceptibility, and security.

Chapter 4

Proposed Gray Image Watermarking

Watermark strength can be controlled by scaling (multiplying) watermark with some suitable scaling factor before embedding [22]. Finding the appropriate values for scaling factor for different types of images is difficult task [22]. In the proposed scheme the HVS and FIS are used to find the adaptive scaling factor for each individual pixel.

4.1 Preparation of Weights

Human eye is less sensitive to changes in textured area as compared to smooth area of an image [32], [33]. So watermark with high, average, and small scaling factor can be embedded in high, medium, small textured areas respectively of an image. Darkness is more tolerable then brightness to watermark [?], so in dark areas watermark with large scaling factor will be added, and in bright areas scaling factor should be small, whereas in middle range of gray levels, medium values of scaling factor will be used. To achieve adaptive scaling factor, FIS is used.

4.1.1 Luminance Masking

Luminance masking is calculated using the procedure given in [?]. The procedure of calculating luminance masking is summarized as following

$$\begin{aligned}
M_L(x,y) &= max\{f_1(bg(x,y), mg(x,y)), f_2(bg(x,y))\} \qquad (4.1)\\
f_1(bg(x,y), mg(x,y)) &= mg(x,y)\alpha(bg(x,y)) + \beta(bg(x,y)),\\
f_2(bg(x,y)) &= \begin{cases} T_o\left(1-\left(\frac{bg(x,y)}{127}\right)^{0.5}\right)+3, & bg(x,y) \leq 127,\\ \gamma(bg(x,y)-127)+3, & bg(x,y) > 127,\end{cases}\\
\alpha(bg(x,y)) &= 0.0001bg(x,y) + 0.115,\\
&\quad 0 \leq x < H, 0 \leq y < W,\\
\beta(bg(x,y)) &= \lambda - 0.01bg(x,y),\\
&\quad 0 \leq x < H, 0 \leq y < W,
\end{aligned}$$

where M_L is the luminance masking, f_1 is the spatial masking function. $bg(x,y)$ is the background luminance and $mg(x,y)$ is the maximum weighted average of luminance differences around the pixel at location (x,y). H and W indicate the image height and width. f_2 is the visibility function based on the background luminance. The parameter α and β are the background luminance dependent functions. The value of some other parameters are: $T_0 = 17, \gamma = 3/128, \lambda = 1/2$.

$mg(x,y)$ and $bg(x,y)$ will be calculated as follows:

$$\begin{aligned}
mg(x,y) &= \max_{k=1,2,3,4}\{|grad_k(x,y)|\},\\
grad_k(x,y) &= \frac{1}{16}\sum_{i=1}^{5}\sum_{j=1}^{5} p(x-3+i, y-3+j)G_k(i,j),\\
&\quad 0 \leq x < H, 0 \leq y < W,
\end{aligned}$$

$$\begin{aligned}
bg(x,y) &= \frac{1}{32}\sum_{i=1}^{5}\sum_{j=1}^{5} p(x-3+i, y-3+j)B(i,j),\\
&\quad 0 \leq x < H, 0 \leq y < W.
\end{aligned}$$

where $p(x, y)$ is the pixel value at the position (x, y), H and W represent the image block size. The values of G_1, G_2, G_3, G_4 and B are given as

$$G_1 = \begin{pmatrix} 0 & 0 & 0 & 0 & 0 \\ 1 & 3 & 8 & 3 & 1 \\ 0 & 0 & 0 & 0 & 0 \\ -1 & -3 & -8 & -3 & -1 \\ 0 & 0 & 0 & 0 & 0 \end{pmatrix}, \quad G_2 = \begin{pmatrix} 0 & 0 & 1 & 0 & 0 \\ 0 & 8 & 3 & 0 & 0 \\ 1 & 3 & 0 & -3 & -1 \\ 0 & 0 & -3 & -8 & 0 \\ 0 & 0 & -1 & 0 & 0 \end{pmatrix}$$

$$G_3 = \begin{pmatrix} 0 & 0 & 1 & 0 & 0 \\ 0 & 0 & 3 & 8 & 0 \\ -1 & -3 & 0 & 3 & 1 \\ 0 & -8 & -3 & 0 & 0 \\ 0 & 0 & 1 & 0 & 0 \end{pmatrix}, \quad G_4 = \begin{pmatrix} 0 & 1 & 0 & -1 & 0 \\ 0 & 3 & 0 & -3 & 0 \\ 0 & 8 & 0 & -8 & 0 \\ 0 & 3 & 0 & -3 & 0 \\ 0 & 1 & 0 & -1 & 0 \end{pmatrix}$$

$$B = \begin{pmatrix} 1 & 1 & 1 & 1 & 1 \\ 1 & 2 & 2 & 2 & 1 \\ 1 & 2 & 0 & 2 & 1 \\ 1 & 2 & 2 & 2 & 1 \\ 1 & 1 & 1 & 1 & 1 \end{pmatrix}$$

4.1.2 Texture Masking

The texture masking values are calculated by using the procedure described in [?] as follows:

$$T_M = |x(i, j) - \overline{x}(i, j)| \tag{4.2}$$

$$\overline{x}(i, j) = \frac{1}{(2L+1)^2} \sum_{k=-L}^{L} \sum_{l=-L}^{L} x(i+k, j+l)$$

A sliding window of size 3×3 will be used, $x(i,j)$ is the pixel value and $\overline{x}(i,j)$ is the mean value at location (i,j) . T_M is the texture masking, and $(2L+1)^2$ represents the pixels in the image block.

4.1.3 Fuzzy Inference System

In the proposed scheme Mamdani fuzzy inference system [34] is used to find the adaptive scaling factor β for (LL band) and γ for (LH, HL, and HH) bands using luminance masking (calculated in eq. 4.1) and texture masking (using eq. 4.2) respectively. The membership functions for luminance masking and texture masking are shown in Figure. 4.1 and Figure. 4.2 respectively. where the values A, B, C, D and E are calculated as

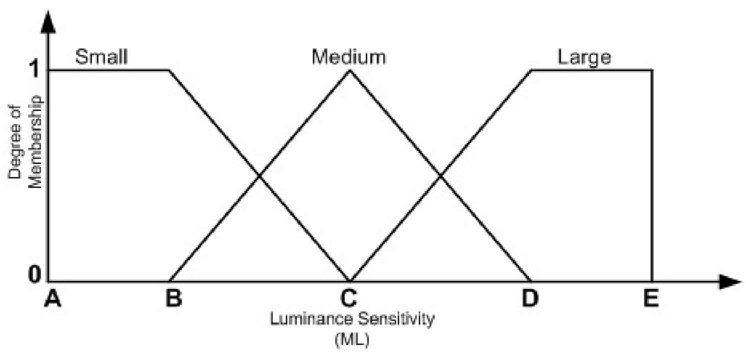

Figure 4.1: Membership Function for Luminance Masking

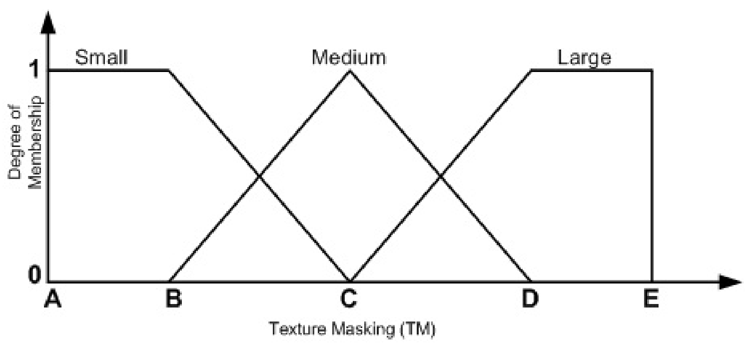

Figure 4.2: Membership Function for Texture Masking

follows:

$$A = \min_{i=1}^{M} \min_{j=1}^{N} (M_L) \tag{4.3}$$

$$C = \frac{1}{MN} \sum_{i=1}^{M} \sum_{j=1}^{N} M_L(i,j) \tag{4.4}$$

$$E = \max_{i=1}^{M} \max_{j=1}^{M} M_L(i,j) \tag{4.5}$$

The values of B such that $(A < B < C)$ and D such that $(C < D < E)$ are calculated in such a way that following condition must be satisfied:

$$C - B = D - C$$

Note that in given case membership function of type triangular and trapezoidal are used, but any type of membership function can be used depending on the requirement. To calculate the values of A, C and E for texture masking use T_M (obtained from eq. 4.2) in eq. 4.3-4.5. The membership function for adaptive strength factor β and γ are shown in Figure. 4.3 and Figure. 4.4 respectively. β and γ are the matrices used as watermark strength factor.

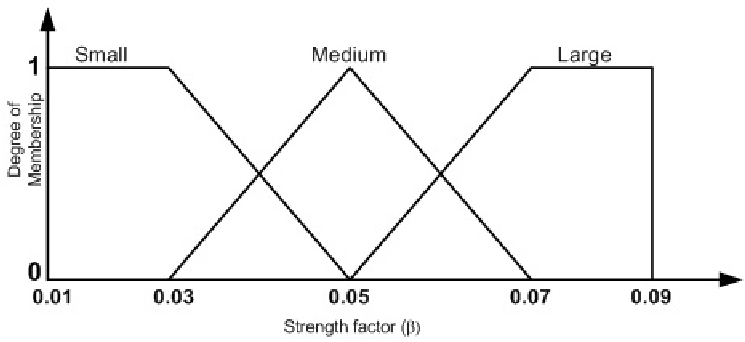

Figure 4.3: Membership Function for β

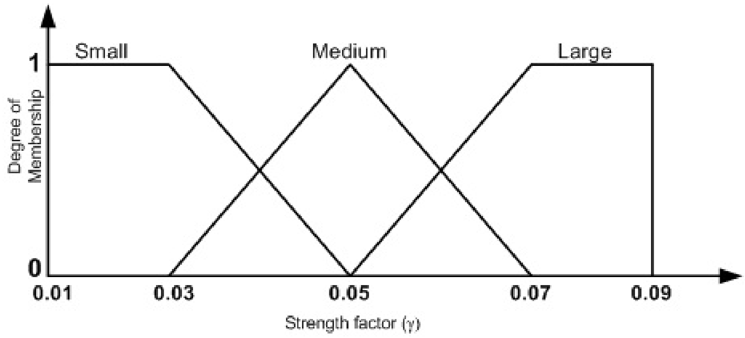

Figure 4.4: Membership Function for γ

Three rules used for calculating β are as follows:

$$Ru^1 : IF\ M_L\ is\ large,\ THEN\ \beta\ is\ large$$
$$Ru^2 : IF\ M_L\ is\ medium,\ THEN\ \beta\ is\ medium$$
$$Ru^3 : IF\ M_L\ is\ small,\ THEN\ \beta\ is\ small$$

Rules for calculating γ are as follows:

$$Ru^1 : IF\ T_M\ is\ large,\ THEN\ \gamma\ is\ large$$
$$Ru^2 : IF\ T_M\ is\ medium,\ THEN\ \gamma\ is\ average$$
$$Ru^3 : IF\ T_M\ is\ small,\ THEN\ \gamma\ is\ small$$

4.2 Watermark embedding:

Use one-level Haar DWT to decompose the cover image I into four sub-bands (i.e., LL, LH, HL, and HH).

$$(LL, LH, HL, HH) = DWT(I)$$

The use of DWT here is to improve the security level and robustness [9], [20]. The improvement in the security level and robustness is due to irregular distribution of watermark over the image during the inverse transform. Apply SVD to LL, LH, HL and

HH sub-bands, i.e.

$$\begin{aligned} U^1S^1V^{1T} &= svd(LL) \\ U^2S^2V^{2T} &= svd(LH) \\ U^3S^3V^{3T} &= svd(HL) \\ U^4S^4V^{4T} &= svd(HH) \end{aligned}$$

where S^1, S^2, S^3 and S^4 are diagonal matrices and contains singular values in descending order.

Modify the singular values in all sub-bands with the watermark image and then apply SVD to them, respectively, i.e.,

$$\begin{aligned} S^1 + \alpha\beta W &= U_W^1 S_W^1 V_W^{1T} \\ S^2 + \alpha\gamma\left(\frac{W}{2}\right) &= U_W^2 S_W^2 V_W^{2T} \\ S^3 + \alpha\gamma\left(\frac{W}{2}\right) &= U_W^3 S_W^3 V_W^{3T} \\ S^4 + \alpha\gamma W^k &= U_W^4 S_W^4 V_W^{4T} \end{aligned} \tag{4.6}$$

where S_w^1, S_w^2, S_w^3 and S_w^4 are diagonal matrices and contain singular values in descending order, W is the watermark and α is the constant strength factor, β is the adaptive scaling factor due to luminance masking and γ is the adaptive scaling factor due to texture masking obtained from FIS.

(LH, HL, and HH) bands represents the texture of an image [28], so texture masking will be used to find adaptive scaling factor for these bands. Where as LL represents the image, so luminance masking is used to calculate the adaptive strength factor for this band. Obtain the sets of modified DWT coefficients, i.e.,

$$LL_W = U^1 S_W^1 V^{1T}$$
$$LH_W = U^2 S_W^2 V^{2T}$$
$$HL_W = U^3 S_W^3 V^{3T}$$
$$HH_W = U^4 S_W^4 V^{4T}$$

Obtain the watermarked image I^W by performing the inverse DWT using modified DWT coefficients.

4.3 Watermark extraction:

Use one-level Haar DWT to decompose the watermarked (possibly distorted) image $\hat{I}_w$ into four subbands (LL, LH, HL, and HH) Apply SVD to all sub-bands, i.e.

$$\hat{LL}_w = \hat{U}^1 \hat{S}_W^1 \hat{V}^{1T}$$
$$\hat{LH}_w = \hat{U}^2 \hat{S}_W^2 \hat{V}^{2T}$$
$$\hat{HL}_w = \hat{U}^3 \hat{S}_W^3 \hat{V}^{3T}$$
$$\hat{HH}_w = \hat{U}^4 \hat{S}_W^4 \hat{V}^{4T}$$

Extract half of the watermark image from each sub-band, i.e.

watermark extracted from LL band

$$W^1 = \left(\frac{U_W^1 \hat{S}_W^1 V_W^{1T} - S^1}{\alpha\beta} \right) \tag{4.7}$$

watermark extracted from LH and HL bands

$$
\begin{aligned}
W^2 &= \left(\frac{U_W^2 \hat{S}_W^2 V_W^{2T} - S^2}{\alpha\gamma}\right) \\
W^3 &= \left(\frac{U_W^3 \hat{S}_W^3 V_W^{3T} - S^3}{\alpha\gamma}\right)
\end{aligned} \tag{4.8}
$$

Add these two watermarks to get the watermark obtained from LH and HL band.

$$W^{23} = W^2 + W^3$$

watermark extracted from HH band

$$W^4 = \left(\frac{U_W^4 \hat{S}_W^4 V_W^{4T} - S^4}{\alpha\gamma}\right) \tag{4.9}$$

In eq. 4.7-4.9, the inverse of matrix β, and γ should be taken element vise not the inverse of whole matrix. The watermark with highest strength factor will be selected.

Chapter 5

Results and Analysis

In this chapter, the results of proposed schemes for different image, different scaling factors and compared with existing state-of-the-art schemes are presented.

5.1 Performance Evaluation

A watermarking scheme is useful if it satisfies two requirements: robustness and imperceptibility. The robustness is measured using NC given in eq. 5.1 and imperceptibility is measured using PSNR given in eq. 5.2.

$$NC = \frac{\sum_{k=1}^{K}\sum_{l=1}^{L}\left(W(k,l) \times \hat{W}(k,l)\right)}{\sqrt{\sum_{k=1}^{K}\sum_{l=1}^{L} W^2(k,l)}\sqrt{\sum_{k=1}^{K}\sum_{l=1}^{L} \hat{W}^2(k,l)}} \tag{5.1}$$

$$PSNR(db) = 10\log_{10}\left(\frac{G^2}{\frac{1}{M\times N}\sum_{m=1}^{M}\sum_{n=1}^{N}(I(m,n) - I_w(m,n))^2}\right) \tag{5.2}$$

where G is the maximum possible intensity value.

5.1.1 Analysis of Proposed Scheme 1

To find out the appropriate bands for watermark embedding several experiments were performed. In these experiments a color image (of size 256×256) and a watermark (of size 128×128). One level DWT decomposition was performed on cover image. Singular values of selected bands were modified for watermark embedding. The detail procedure for embedding and extraction is discussed in coming section.

In scheme P1, the first principal component (PC) was selected for embedding watermark. Different bands were chosen for watermark embedding.IN scheme P1a, same watermark is embedded into all bands after one level DWT decomposition (i.e. LL, LH, HL, and HH). After extraction one watermark (with largest NC) out of four is selected. In scheme P1b, watermark is embedded into (LH and HL) bands of cover image after one level DWT decomposition. The watermark with highest NC will be selected.

In scheme P1c, the full watermark is embedded in (LL and HH) bands separately, whereas half of the watermark is embedded into (LH and HL) bands. It means three watermarks will be extracted, and the watermark with highest NC will be selected.

In scheme P1d, Watermark is divided into half and each half is embedded into (LH and HL) and (LL and HH) bands. In scheme P1e, complete watermark is embedded into LL band and in (LH and HL) bands half of the watermark is embedded.

The results in terms of NC are shown in Table 5.1 and in terms of PSNR in Table 5.2.

Table 5.1: NC for different cases of schemes P1 ($\alpha = 0.3$)

Attacks	Scheme P1a	Scheme P1b	Scheme P1c	Scheme P1d	Scheme P1e
HISTOGRAM EQUALIZATION	0.6241	0.2238	0.6241	0.2238	0.6241
ROTATION	0.8395	0.6305	0.8193	0.6305	0.8193
GAUSSIAN NOISE	0.5471	0.2241	0.5544	0.3102	0.4774
SCALING	0.6813	0.4681	0.5139	0.4682	0.4682
CROPPING	0.2467	0.1406	0.1406	0.1406	0.1406
JPEG COMPRESSION	0.8506	0.5583	0.8505	0.5998	0.5583
Y-SHEARING	0.8221	0.8634	0.8634	0.8634	0.8634
X-SHEARING	0.8056	0.7119	0.8056	0.7119	0.8056
MEDIAN FILTERING	0.2443	0.1336	0.2443	0.1398	0.2443
AFFINE TRANSFORMATION	0.7085	0.7435	0.7434	0.7435	0.7435
TRANSLATION	0.9105	0.6674	0.6674	0.6674	0.6674
SALT AND PEPPER	0.4402	0.1850	0.4412	0.2705	0.4407
SHARPENING	0.4132	0.1501	0.4132	0.1688	0.4132
BLURRING	0.2185	0.1419	0.1534	0.1419	0.1419
AVERAGING FILTER	0.1412	0.0756	0.1412	0.0756	0.0756

IN scheme P2, the second PC was selected for embedding watermark. Different bands

Table 5.2: PSNR for different cases of schemes P1 ($\alpha = 0.3$)

	Scheme P1a	Scheme P1b	Scheme P1c	Scheme P1d	Scheme P1e
PSNR	77.3193	92.3562	78.4661	87.0874	81.7726

were chosen for watermark embedding.

In scheme P2a, same watermark is embedded into all bands after one level DWT decomposition (i.e. LL, LH, HL, and HH). After extraction one watermark (with largest NC) out of four will be selected.

In scheme P2b, watermark is embedded into (LH and HL) bands of cover image after one level DWT decomposition. The watermark with highest NC will be selected.

In scheme P2c, the full watermark is embedded in (LL and HH) bands separately, whereas half of the watermark is embedded into (LH and HL) bands. It means three watermarks will be extracted, and the watermark with highest NC will be selected.

In scheme P2d, watermark is divided into half and each half is embedded into (LH and HL) and (LL and HH) bands. In scheme P2e, complete watermark is embedded into LL band and in (LH and HL) bands half of the watermark is embedded.

The results in terms of NC are shown in Table 5.3 and in terms of PSNR in Table 5.4.

Table 5.3: NC for different cases of schemes P2 ($\alpha = 0.3$)

Attacks	Scheme P2a	Scheme P2b	Scheme P2c	Scheme P2d	Scheme P2e
HISTOGRAM EQUALIZATION	0.8012	0.2238	0.8012	0.5551	0.8012
ROTATION	0.7776	0.6305	0.6370	0.5849	0.6368
GAUSSIAN NOISE	0.6370	0.2268	0.6370	0.4357	0.6363
SCALING	0.7372	0.4681	0.7372	0.6123	0.6123
CROPPING	0.4124	0.1406	0.2889	0.2375	0.2375
JPEG COMPRESSION	0.8559	0.5583	0.8560	0.8320	0.7751
Y-SHEARING	0.8283	0.8634	0.7316	0.6398	0.7315
X-SHEARING	0.8463	0.7119	0.7941	0.7941	0.7940
MEDIAN FILTERING	0.5410	0.1336	0.5120	0.3522	0.5118
AFFINE TRANSFORMATION	0.7567	0.7435	0.6181	0.5767	0.6179
TRANSLATION	0.7934	0.6674	0.7845	0.7843	0.7844
SALT AND PEPPER	0.6290	0.1839	0.6290	0.4175	0.6297
SHARPENING	0.7566	0.1501	0.7566	0.4599	0.7567
BLURRING	0.3748	0.1419	0.3376	0.1900	0.1874
AVERAGING FILTER	0.3339	0.0756	0.3092	0.1731	0.1618

Table 5.4: PSNR for different cases of schemes P2 ($\alpha = 0.3$)

	Scheme P2a	Scheme P2b	Scheme P2c	Scheme P2d	Scheme P2e
PSNR	73.9656	95.3689	76.1954	82.5542	81.5729

In scheme P3, the third PC was selected for embedding watermark. Different bands were chosen for watermark embedding like:

IN scheme P3a, same watermark is embedded into all bands after one level DWT decomposition (i.e. LL, LH, HL, and HH). After extraction one watermark (with largest NC) out of four will be selected.

In scheme P3b, watermark is embedded into (LH and HL) bands of cover image after one level DWT decomposition. The watermark with highest NC will be selected.

In scheme P3c, the full watermark is embedded in (LL and HH) bands separately, whereas half of the watermark is embedded into (LH and HL) bands. It means three watermarks will be extracted, and the watermark with highest NC will be selected.

In scheme P3d, watermark is divided into half and each half is embedded into (LH and HL) and (LL and HH) bands. In scheme P3e, complete watermark is embedded into LL band and in (LH and HL) bands half of the watermark is embedded.

The results in terms of NC are shown in Table 5.5 and in terms of PSNR in Table 5.6.

Comparing results using different options of watermark embedding, it reveals, that embedding watermark in first principal component (scheme P1) gives better results as compared to schemes P2 and P3. More precisely, scheme P1c performs well as compared to all other options.

Various experiments were performed to explore the consequences of embedding and extraction of watermark into the color images. For this purpose, color images of size (512×512) and gray watermark (logo) (128×128) were chosen as shown in Figure 5.1.

Various attacks (histogram equalization, rotation, Gaussian noise, scaling, cropping, JPEG compression, Y-shearing, X-shearing, median filtering, affine transformation, translation, salt & pepper, sharpening, blurring, average filtering) were applied on watermarked image to evaluate the performance of purposed scheme. The extracted watermark

Table 5.5: NC for different cases of schemes P3 ($\alpha = 0.3$)

Attacks	Scheme P3a	Scheme P3b	Scheme P3c	Scheme P3d	Scheme P3e
HISTOGRAM EQUALIZATION	0.8439	0.2238	0.8118	0.7632	0.8118
ROTATION	0.6848	0.6305	0.6951	0.6949	0.6951
GAUSSIAN NOISE	0.7035	0.2254	0.7027	0.5502	0.7016
SCALING	0.7268	0.4681	0.7459	0.7454	0.7455
CROPPING	0.5654	0.1406	0.5208	0.5208	0.5208
JPEG COMPRESSION	0.7952	0.5583	0.8223	0.8595	0.8221
Y-SHEARING	0.7894	0.8634	0.7173	0.7167	0.7165
X-SHEARING	0.8127	0.7119	0.8093	0.8090	0.8090
MEDIAN FILTERING	0.6765	0.1336	0.6767	0.6275	0.6753
AFFINE TRANSFORMATION	0.7143	0.7435	0.6976	0.6969	0.6967
TRANSLATION	0.7704	0.6674	0.8162	0.8161	0.8160
SALT AND PEPPER	0.7056	0.1826	0.7059	0.5355	0.7038
SHARPENING	0.8122	0.1501	0.8124	0.7199	0.8122
BLURRING	0.4943	0.1419	0.4943	0.3887	0.3887
AVERAGING FILTER	0.4747	0.0756	0.4746	0.3470	0.3469

Table 5.6: PSNR for different cases of schemes P3 ($\alpha = 0.3$)

	Scheme P3a	Scheme P3b	Scheme P3c	Scheme P3d	Scheme P3e
PSNR	69.8743	95.2356	70.3887	77.8240	77.0356

are shown in Figure 5.2

The result in terms of NC and PSNR for different level of DWT decomposition are shown in Table 5.7 (using Lena image) and Table 5.8 (using different images) respectively. Note that, with increase in level, the imperceptibility improves. Therefore, we use second level DWT for following simulations.

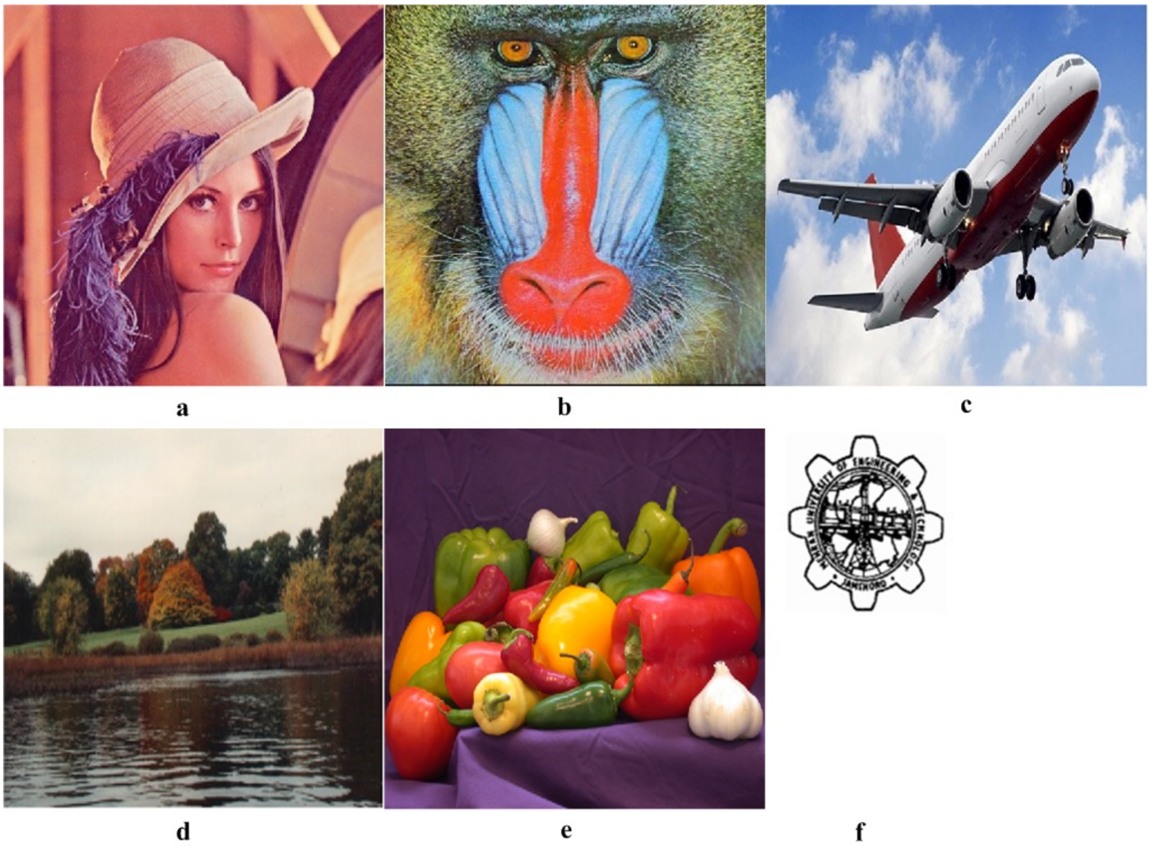

Figure 5.1: (a). Lena, (b). Baboon, (c). Aeroplane, (d). Autumn, (e). Peppers (f). Watermark(logo)

The performance of proposed scheme in terms of PSNR is shown in Table 5.9 (using different images), and in terms of NC is shown in Table 5.10 (using Lena image), for different strength factor (i.e. α).

It is clear from values that larger strength factor, provides better robustness where as smaller strength factor gives good imperceptibility result.

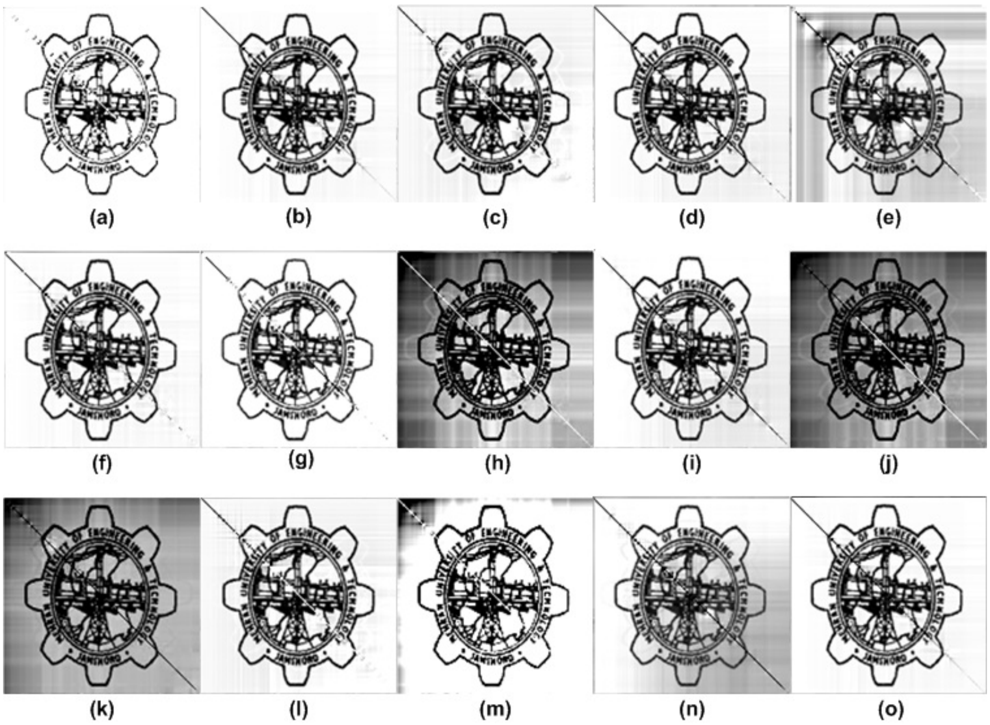

Figure 5.2: (a). Histogram Equalization, (b). Rotation, (c). Gaussian Noise, (d). Scaling, (e). Cropping, (f). JPEG Compression (g). Y-shearing (h). X-shearing, (i). Median Filtering, (j). Affine Transformation, (k). Translation, (l). Salt & Pepper, (m). Sharpening (n). Blurring (o). Average Filtering

Different images are also used to measure the quality of proposed scheme and the result is shown in Table 5.11 .

Table 5.7: NCs for different levels ($\alpha = 0.3$)

Attacks	1^{st} Level	2^{nd} Level	3^{rd} Level
Histogram Equalization	0.8217	0.8381	0.5802
Rotation	0.8045	0.8534	0.8892
Gaussian Noise	0.7894	0.8287	0.8211
Scaling	0.7345	0.8393	0.8776
Cropping	0.5625	0.4918	0.6099
JPEG Compression	0.7554	0.8535	0.8883
Y-Shearing	0.8196	0.8431	0.8607
X-Shearing	0.8309	0.8358	0.7545
Median Filtering	0.7067	0.8307	0.8846
Affine Transformation	0.8218	0.8412	0.7487
Translation	0.8487	0.8968	0.7620
Salt & Pepper	0.7803	0.8227	0.8122
Sharpening	0.8279	0.8578	0.9296
Gaussian Blurring	0.4577	0.6457	0.6868
Averaging Filter	0.8106	0.8534	0.8892

Table 5.8: PSNR for different levels ($\alpha = 0.3$)

Images	1^{st} Level	2^{nd} Level	3^{rd} Level
Lena	55.6232	66.8290	70.9174
Baboon	42.6506	66.8290	68.1598
Aeroplane	54.3406	63.1777	78.3717
Autumn	50.3772	71.1457	69.7282
Peppers	51.1524	62.1909	67.8758

Table 5.12 and Table 5.13 shows the comparison of proposed scheme with the different schemes in terms of NC and PSNR respectively (for Lena image). In this scheme all DWT sub-bands are chosen for watermark embedding, therefore it is very difficult to remove the watermark. Proposed scheme is tested using different strength factor and using different images and it is found that this schemes performs well against many attacks (including histogram equalization, rotation, Gaussian noise, scaling, cropping, JPEG compression Y-shearing, X-shearing, median filtering, affine transformation, translation, salt & pepper, sharpening, blurring, average filtering). Since imperceptibility and robustness are the measure for quality of watermark, and results show that this schemes satisfies both quality measures.

Table 5.9: PSNR for different α

Images	α (0.1)	α (0.3)	α (0.5)	α (0.7)	α (0.9)
Lena	81.3125	66.8290	62.9989	59.4988	56.1143
Baboon	77.9493	66.8290	53.0142	49.7989	48.8085
Aeroplane	84.5347	63.1777	62.0194	59.3736	56.1099
Autumn	74.7727	71.1457	58.6099	55.1685	51.9749
Peppers	75.0462	62.1909	57.6246	54.6487	53.0597

Table 5.10: NC for different α

Attacks	α (0.1)	α (0.3)	α (0.5)	α (0.7)	α (0.9)
Histogram Equalization	0.6002	0.8381	0.8327	0.8145	0.8216
Rotation	0.9371	0.8534	0.8144	0.7987	0.7803
Gaussian Noise	0.7916	0.8287	0.8358	0.8402	0.8330
Scaling	0.8908	0.8393	0.7913	0.7818	0.7695
Cropping	0.2732	0.4918	0.5852	0.6159	0.6243
JPEG Compression	0.9375	0.8535	0.8219	0.8077	0.7933
Y-Shearing	0.8754	0.8431	0.8271	0.8105	0.7935
X-Shearing	0.8110	0.8358	0.8367	0.8237	0.8089
Median Filtering	0.8458	0.8307	0.7759	0.7461	0.7423
Affine Transformation	0.7429	0.8412	0.8483	0.8362	0.8206
Translation	0.8945	0.8968	0.8622	0.8379	0.8189
Salt & Pepper	0.7733	0.8227	0.8434	0.8392	0.8258
Sharpening	0.5188	0.8578	0.8476	0.8268	0.8241
Gaussian Blurring	0.4116	0.6457	0.6650	0.6589	0.6675
Averaging Filter	0.9371	0.8534	0.8207	0.8067	0.7921

5.1.2 Analysis of Proposed Scheme 2

A number of experiments were performed to investigate the effects of embedding and extraction of color watermark into the color images. For this purpose, color images of size (512×512) were chosen. In Figure 5.3, color images and their watermarked versions are shown.

Table 5.11: NCs for different images ($\alpha = 0.3$)

Attacks	Lena	Baboon	Aeroplane	Autumn	Peppers
Histogram Equalization	0.8381	0.8353	0.8152	0.8166	0.8072
Rotation	0.8534	0.8532	0.8330	0.8607	0.8407
Gaussian Noise	0.8287	0.8274	0.8130	0.8111	0.7903
Scaling	0.8393	0.8392	0.8174	0.8452	0.8305
Cropping	0.4918	0.4903	0.2966	0.2749	0.4091
JPEG Compression	0.8535	0.8533	0.8331	0.8585	0.8380
Y-Shearing	0.8431	0.8408	0.7906	0.8316	0.7883
X-Shearing	0.8358	0.8333	0.8154	0.8335	0.7845
Median Filtering	0.8307	0.8306	0.8045	0.8256	0.8181
Affine Transformation	0.8412	0.8387	0.8164	0.7932	0.8059
Translation	0.8968	0.8953	0.9001	0.8429	0.8202
Salt & Pepper	0.8227	0.8211	0.7954	0.8209	0.8152
Sharpening	0.8578	0.8573	0.9054	0.8881	0.9052
Gaussian Blurring	0.6457	0.6459	0.6155	0.6068	0.6857
Averaging Filter	0.8534	0.8532	0.8330	0.8607	0.8407

Various attacks (histogram equalization, rotation, Gaussian noise, scaling, cropping, JPEG compression Y-shearing, X-shearing, median filtering, affine transformation, translation, salt & pepper, sharpening, blurring, average filtering) were applied on watermarked image to evaluate the performance of purposed scheme. The extracted watermark are shown in Figure 5.4

Table 5.12: NC for different Schemes

Attacks	Proposed scheme1	Proposed scheme2	DWT-SVD based [12]	DWT [29]	SVD [9]
Histogram Equalization	0.8381	0.9812	0.6111	0.1453	0.2235
Rotation	0.8534	0.9589	0.2404	0.2372	0.3080
Gaussian Noise	0.8287	0.8832	0.6050	0.2053	0
Scaling	0.8393	0.8835	0.2415	0.2369	0.3080
Cropping	0.4918	0.9107	0.2397	0.2493	0.2051
JPEG Compression	0.8535	0.7796	0.2415	1	1
Y-Shearing	0.8431	0.9143	0.2396	0.1999	0.2164
X-Shearing	0.8358	0.9092	0.5836	0.2148	0.2588
Median Filtering	0.8307	0.5046	0.5249	0.8191	0.2923
Affine Transformation	0.8412	0.8854	0.5162	0.2439	0.2263
Translation	0.8968	0.9157	0.2320	0.2103	0.1917
Salt & Pepper	0.8227	0.8124	0.6028	0.4179	0
Sharpening	0.8578	0.9106	0.6587	0.8457	0.3052
Blurring	0.6457	0.5171	0.4774	0.8018	0.857
Average Filtering	0.8534	0.4369	0.3943	1	1

Table 5.13: PSNR for different schemes

Attacks	Proposed scheme1	Proposed scheme2	DWT-SVD based [12]	DWT [29]	SVD [9]
Lena	66.8290	32.2439	5.1733	42.8330	34.2224

The result in terms of NC and PSNR for different level of DWT decomposition are shown in Table 5.14 (using Lena image) and Table 5.15 (using different images) respectively.

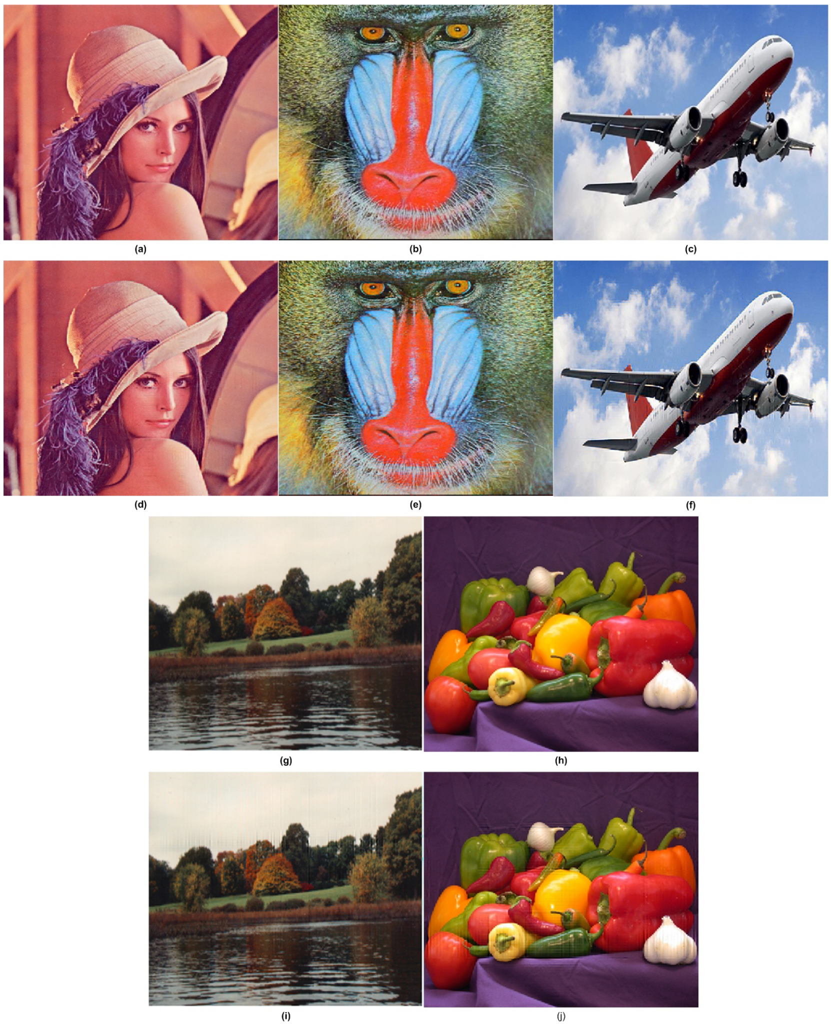

Figure 5.3: (a),(b),(c), (g) and (h) . Original Images (d), (e), (f), (i) and (j). Watermarked Images

The performance of proposed scheme in terms of PSNR is shown in Table 5.16 (using different images), and in terms of NC is shown in Table 5.17 (using Lena image), for different strength factor (i.e. α). It is clear from values that larger strength factor, provides better robustness where as smaller strength factor gives good imperceptibility result.

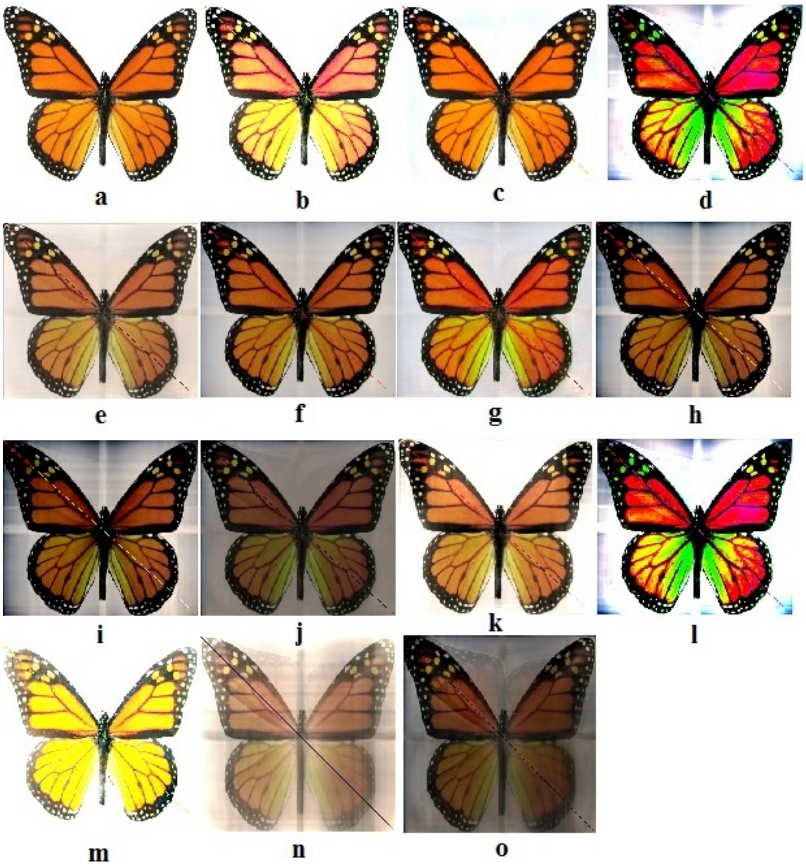

Figure 5.4: (a). Histogram Equalization, (b). Rotation, (c). Gaussian Noise, (d). Scaling, (e). Cropping, (f). JPEG Compression (g). Y-shearing (h). X-shearing, (i). Median Filtering, (j). Affine Transformation, (k). Translation, (l). Salt & Pepper, (m). Sharpening (n). Gaussian Blur (o). Average Filtering

Different images are also used to measure the quality of proposed scheme and the result is shown in Table 5.18 .

Table 5.14: NCs for different levels ($\alpha = 0.09$)

Attacks	1^{st} Level	2^{nd} Level	3^{rd} Level
Histogram Equalization	0.9812	0.9754	0.7610
Rotation	0.9589	0.8430	0.5646
Gaussian Noise	0.8832	0.4730	0.3412
Scaling	0.8835	0.7664	0.6068
Cropping	0.9107	0.9248	0.7301
JPEG Compression	0.7796	0.7679	0.5428
Y-Shearing	0.9143	0.9091	0.7126
X-Shearing	0.9092	0.8485	0.5859
Median Filtering	0.5046	0.3878	0.4195
Affine Transformation	0.8854	0.7739	0.5180
Translation	0.9157	0.9194	0.4055
Salt & Pepper	0.8124	0.4755	0.4113
Sharpening	0.9106	0.9635	0.6368
Gaussian Blur	0.5171	0.4980	0.4729
Average Filtering	0.4369	0.3628	0.3906

Table 5.15: PSNR for different levels ($\alpha = 0.09$)

Images	1^{st} Level	2^{nd} Level	3^{rd} Level
Lena	32.2439	33.2446	31.8695
Baboon	25.1937	27.2996	31.9990
Aeroplane	30.7181	29.3945	27.8570
Autumn	30.7181	28.1863	27.1823
Peppers	34.4122	39.2254	36.8868

5.1.3 Analysis of Proposed Scheme 3

To explore the consequences of using human visual system (luminance masking and texture masking) in embedding and extraction of watermark into gray scale images. A gray scale image (of size 512×512) and a watermark image (of size 256×256) as shown in Figure 5.5 were used.

In Table 5.19, NC against various attacks (Histogram equalization, rotation, Gaussian noise, scaling, cropping, JPEG compression, Y-shearing, X-shearing, median filtering, affine transformation, translation, salt & pepper, sharpening, blurring, average filtering) are shown when adaptive strength factors β (using luminance masking), and γ (using texture masking) were not used.The extracted watermarks without using β and γ in embedding process are shown in Figure 5.6

Table 5.16: PSNR for different α

Images	α (0.01)	α (0.03)	α (0.05)	α (0.07)	α (0.09)
Lena	35.6693	35.3928	34.6003	33.4812	32.2439
Baboon	25.5068	25.4927	25.4421	25.3369	25.1937
Aeroplane	32.2450	32.1853	31.9242	31.4116	30.7181
Autumn	34.0910	33.9672	33.5762	32.9965	30.7181
Peppers	44.9146	43.0919	39.6794	36.7568	34.4122

Table 5.17: NC for different α

Attacks	α (0.01)	α (0.03)	α (0.05)	α (0.07)	α (0.09)
Histogram Equalization	0.9546	0.9813	0.9852	0.9845	0.9812
Rotation	0.4316	0.8043	0.9092	0.9440	0.9589
Gaussian Noise	0.5866	0.8221	0.8638	0.8749	0.8832
Scaling	0.3316	0.6668	0.7358	0.8433	0.8835
Cropping	0.3467	0.6796	0.8233	0.8815	0.9107
JPEG Compression	0.3317	0.3995	0.5803	0.6995	0.7796
Y-Shearing	0.6552	0.8701	0.9103	0.9168	0.9143
X-Shearing	0.5346	0.8240	0.8893	0.9057	0.9092
Median Filtering	0.3317	0.3318	0.3452	0.4387	0.5046
Affine Transformation	0.4773	0.7844	0.8583	0.8793	0.8854
Translation	0.3312	0.7345	0.8642	0.9150	0.9157
Salt & Pepper	0.6379	0.8427	0.8695	0.8569	0.8124
Sharpening	0.3317	0.6193	0.7990	0.8734	0.9106
Gaussian Blur	0.3314	0.3314	0.3776	0.4572	0.5171
Average Filtering	0.3317	0.3317	0.3318	0.3679	0.4369

In Table 5.20, NC against various attacks (Histogram equalization, rotation, Gaussian noise, scaling, cropping, JPEG compression, Y-shearing, X-shearing, median filtering, affine transformation, translation, sharpening, blurring, average filtering) are shown when adaptive strength factors β (using luminance masking), and γ (using texture masking) were used.

Table 5.18: NCs for different images ($\alpha = 0.09$)

Attacks	Lena	Baboon	Aeroplane	Autumn	Peppers
Histogram Equalization	0.9660	0.7400	0.8605	0.9738	0.9812
Rotation	0.7799	0.8785	0.9547	0.9940	0.9589
Gaussian Noise	0.3912	0.6944	0.7191	0.8210	0.8832
Scaling	0.7420	0.8537	0.9395	0.9345	0.8835
Cropping	0.4283	0.7844	0.7574	0.9366	0.9107
JPEG Compression	0.5491	0.7037	0.8231	0.9611	0.7796
Y-Shearing	0.4632	0.8169	0.6291	0.8998	0.9143
X-Shearing	0.5835	0.8546	0.6017	0.9252	0.9092
Median Filtering	0.3317	0.4680	0.4250	0.8898	0.5046
Affine Transformation	0.3318	0.7518	0.5613	0.8697	0.8854
Translation	0.6035	0.8514	0.8824	0.9475	0.9157
Salt & Pepper	0.3910	0.6105	0.6770	0.9104	0.8124
Sharpening	0.5408	0.9255	0.9431	0.9868	0.9106
Gaussian Blur	0.3317	0.3554	0.4921	0.8483	0.5171
Average Filtering	0.3317	0.3318	0.4336	0.8268	0.4369


(a) (b)

Figure 5.5: (a). Lena, (b). Watermark

The extracted watermark using HVS are shown in Figure 5.7

Table 5.19: NC for different strength factors using Lena image

ATTACKS	0.1	0.3	0.5	0.7	0.9
Histogram Equalization	0.9562	0.9744	0.9708	0.9716	0.9640
Rotation	0.7714	0.7003	0.7731	0.8434	0.8879
Gaussian Noise	0.5664	0.8949	0.9582	0.9637	0.9528
Scaling	0.9519	0.9930	0.9946	0.9900	0.9761
Cropping	0.5755	0.8733	0.9099	0.9182	0.9191
JPEG Compression	0.9992	0.9975	0.9935	0.9840	0.9666
Y-shearing	0.8726	0.8459	0.8243	0.8077	0.7956
X-shearing	0.8477	0.8128	0.7821	0.7606	0.7441
Median Filtering	0.6968	0.9352	0.9709	0.9807	0.9796
Affine Transformation	0.8272	0.7751	0.7335	0.7077	0.6901
Translation	0.9081	0.9493	0.9578	0.9732	0.9706
Salt and Pepper	0.8300	0.9785	0.9884	0.9835	0.9688
Sharpening	0.8856	0.9440	0.9375	0.9256	0.9148
Gaussian Blurring	0.4917	0.8564	0.9218	0.9329	0.9252
Averaging Filter	0.4454	0.8284	0.9057	0.9209	0.9152

In Table 5.21, PSNR (using Lena image and $\alpha = 0.9$) are shown. In Figure 5.8, watermarked Lena images using HVS and without using HVS are shown.

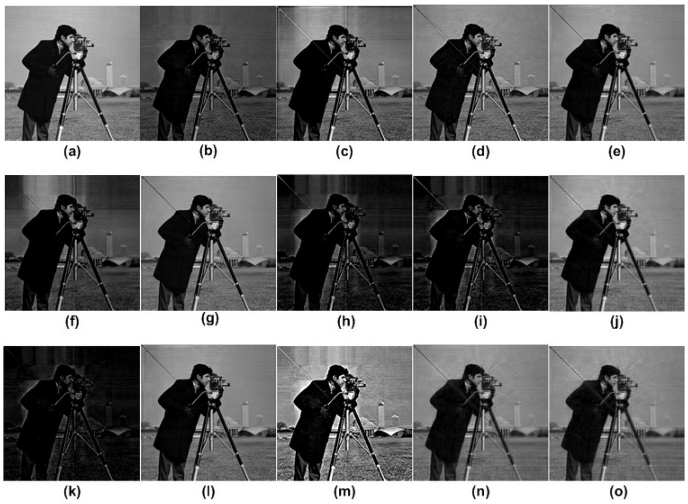

Figure 5.6: (a). Histogram Equalization (b). Gaussian Noise (c). Rotation, (d). Scaling (e). Cropping (f). JPEG Compression, (g). Y-Shearing (h). X-Shearing (i). Median Filtering (j). Affine Transformation (k). Translation (l). Salt & Pepper (m). Sharpening (n). Blurring (o). Average Filtering

It can be seen from Figure 5.8 that using HVS improves the PSNR significantly. The statistical result of NC shown in Table 5.20 are comparatively less than the values given in Table 5.19 but from Figure. 5.6 and Figure. 5.7, it is clearly seen that the extracted watermarks are visually good in both the cases (with HVS and without HVS).

5.2 Conclusion

The experimental results of proposed schemes were presented in this chapter. It is found that proposed schemes performs well, specially in terms of imperceptibility and also robust against most of the attacks.

Table 5.20: NC for different scaling factors using Lena image

ATTACKS	0.1	0.3	0.5	0.7	0.9	1
Histogram Equalization	0.4050	0.5336	0.7222	0.8173	0.8702	0.8885
Rotation	0.4010	0.4040	0.3906	0.3941	0.3986	0.3971
Gaussian Noise	0.4123	0.4371	0.5437	0.6278	0.6788	0.6962
Scaling	0.4122	0.4120	0.5911	0.7189	0.8548	1.0000
Cropping	0.4123	0.4122	0.4122	0.4122	0.4122	0.4122
JPEG Compression	0.8032	0.9700	0.9877	0.9920	0.9948	0.9958
Y-shearing	0.5587	0.8762	0.9047	0.8886	0.8758	0.8716
X-shearing	0.4123	0.5428	0.6866	0.7429	0.7710	0.7801
Median Filtering	0.4122	0.4121	0.4121	0.4120	0.4266	0.4601
Affine Transformation	0.4700	0.6901	0.7173	0.7254	0.7566	0.7663
Translation	0.4305	0.7118	0.7901	0.8149	0.8296	0.8354
Salt & Pepper	0.4121	0.4120	0.4118	0.4117	0.4116	0.4116
Sharpening	0.3678	0.3724	0.4964	0.6141	0.7010	0.7333
Gaussian Blurring	0.4122	0.4123	0.4123	0.4122	0.4122	0.4121
Averaging Filter	0.4122	0.4122	0.4122	0.4122	0.4121	0.4121

Table 5.21: PSNR for $\alpha = 0.9$

Schemes	0.1	0.3	0.5	0.7	0.9
Without FIS	31.0639	21.9681	18.1268	15.7270	14.1259
With FIS	70.1466	50.9989	45.1251	41.4769	38.8361

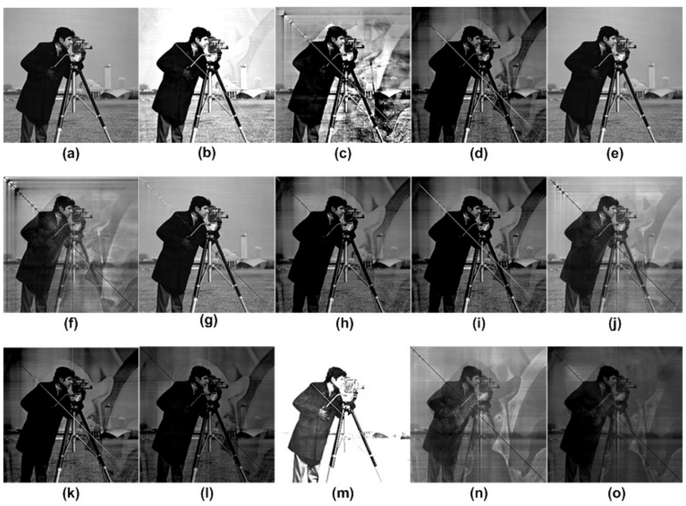

Figure 5.7: (a). Histogram Equalization (b). Gaussian Noise (c). Rotation, (d). Scaling (e). Cropping (f). JPEG Compression, (g). Y-Shearing (h). X-Shearing (i). Median Filtering (j). Affine Transformation (k). Translation (l). Salt & Pepper (m). Sharpening (n). Blurring (o). Average Filtering

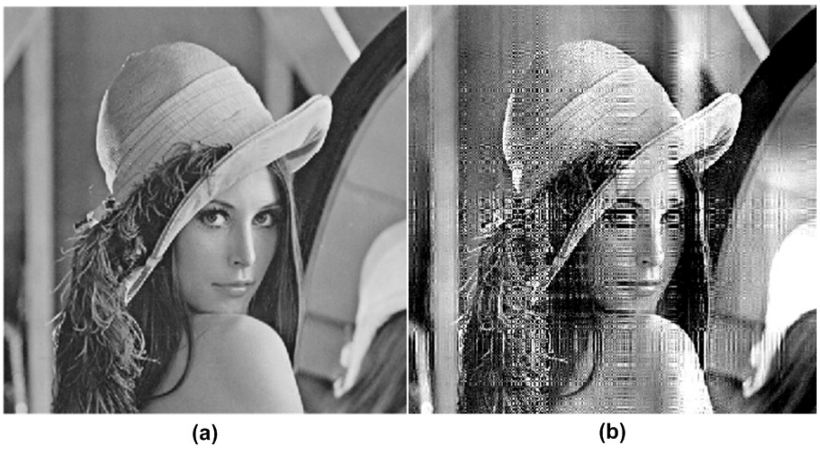

Figure 5.8: (a). Using HVS (b). Without using HVS

Chapter 6

Conclusion and Future Work

In this chapter, the contribution of our work and possible future work are discussed.

6.1 Conclusion

In this thesis three schemes are proposed for image watermarking.

In the first scheme, a gray watermark was embedded into a color image. The three highly correlated channels (R, G and B) are uncorrelated using PCA. The first principal component (which contains the most of the information) is decomposed into (LL, LH, HL and HH) bands using 2-level Haar DWT. The gray watermark is introduced into singular values of all bands (i.e., LL, LH, HL and HH). This scheme satisfies both the requirements (imperceptibility and robustness) of watermarking significantly.

In the second scheme, a color watermark is embedded into a color image. The PCA is used to un-correlate the three channels (R, G and B) of both (i.e. watermark and cover image). The one level DWT is performed to decompose all the principal components of cover image into (LL, LH, HL and HH) bands. The SVD of (LH and HL) band is performed on all principal components. The principal component of corresponding channel of watermark is introduced into the singular values of corresponding channel of cover image. As in this scheme more information is embedded into the cover image, so it difficult for intentional or unintentional attacker to remove the watermark. Given scheme is imperceptible and robust.

In the third scheme a gray watermark is embedded into gray cover image. One of the greatest challenge with existing watermarking schemes is to choose the appropriate scaling factor for watermark embedding. In this scheme, luminance masking and texture masking are exploited to achieve the adaptive scaling factor for each pixel with the help of FIS. The pixel with large luminance masking value can tolerate watermark with large scaling factor without visible degradation, and pixel with small luminance masking value value needs small scaling factor. Similarly, with large texture value, large scaling factor can be used to embed to the watermark and pixel with small texture value, requires small scaling factor for watermark embedding. In this way a watermarking scheme with better imperceptibility and robustness can be achieved.

6.2 Future Work

In proposed work, watermarking schemes for images is presented, it can be extended for audio and video watermarking. A program can be embedded into audio or video files, which when detected by the player will disable the copy option, consequently solving the issue of illegal copying.

Bibliography

[1] J. C. Ingemar, L. M. Matthew, A. B. Jeffrey, "Introduction" in *Digital Watermarking,* 1^{st} ed. Morgan Kaufmann, pp. 1-9, 2001.

[2] C. Q. Yin, L. Li, A. Q. Lv, L. Qu, "A Color Image Watermarking Algorithm Based on DWT-SVD," *IEEE Int. Conf. on Automation and Logistics,* pp. 2607-2611, Aug, 2007.

[3] S. Rawat, B. Raman, "A new robust watermarking scheme for color images," *IEEE Int. Conf. on Advance Computing,* pp. 206-209, 2010.

[4] V. Santhi, N. Rekha, S. Tharini, "A hybrid block based watermarking algorithm using DWT-DCT-SVD techniques for color images," *Int. Conf. on Computing, Communication and Networking,* pp. 1-7, Dec, 2008.

[5] C. S. Lu, "Multimedia Security: Steganography and Digital Watermarking Techniques for Protection of Intellectual Property," 1^{st}*ed.* Idea Group, pp. 1-47, 2005.

[6] S. P. Mohanty, K. R. Ramakrishnan, M. S. Kankanhalli, "A DCT domain visible watermarking technique for images," *IEEE Int. Conf on Multimedia and Expo,* pp. 1029-1032, 2000.

[7] E. Ganic, A. M. Eskicioglu, "Robust DWT-SVD Domain Image Watermarking: Embedding Data in All Frequencies," *In Proc. of the workshop on Multimedia and security,* pp. 166-174, 2004.

[8] S. Ramakrishnan, T. Gopalakrishnan, K. Balasamy, "A wavelet based hybrid svd

algorithm for digital image watermarking," *Int. Journal of Signal & Image Processing,* vol.2, n.3, pp. 157-174, September, 2011.

[9] V.Santhi, A. Thangavelu, "DWT-SVD combined full band robust watermarking technique for color images in YUV color space," *Int. Journal of Computer Theory and Engineering,* Vol. 1, No. 4, pp. 1793-8201, October 2009.

[10] M. J. Tsai, C. C. Chien, "A wavelet-based semi-fragile watermarking with recovery mechanism," *IEEE Int. Symposium on Circuits and Systems,* pp. 3033-3036, 2008.

[11] W. Yongqi, Z. hui, "A color image blind watermarking algorithm based on chaotic scrambling and integer wavelet,", *IEEE Int. Conf. on Network Computing and Information Security,* pp. 413-416, 2011.

[12] X. You, L. Du, Y. M. Cheung, Q. Chen, "A blind watermarking scheme using new nontensor product wavelet filter banks," *IEEE Trans. on Image Processing*, vol. 19, no. 12, pp. 3271-3284 December, 2010.

[13] R. Nia, Q. Ruana, H.D. Chengb, "Secure semi-blindwatermarking based on iteration mapping and image features," *Int. Journal of Pattern Recognition* vol. 38, issue. 3, pp. 357-368, March, 2005.

[14] C. C. Lai, C. C. Tsai, "Digital Image Watermarking Using Discrete Wavelet Transform and Singular Value Decomposition, " *IEEE Trans. on Instrumentation and Measurement,* vol. 59 Issue. 11, pp. 3060-3063 , Nov, 2010

[15] N. V. Dharwadkar, B. B. Amberker, A. Gorai, "Non-blind watermarking scheme for color images in RGB space using DWT-SVD," *IEEE Conf. on Communications and Signal Processing (ICCSP),* pp. 489-493, 2011.

[16] L. Baisa, Gunjal, S. N. Mali, "Comparative performance analysis of DWT-SVD based color image watermarking technique in YUV, RGB and YIQ color spaces," *Int. Journal of Computer Theory and Engineering,* vol. 3, no. 6, pp. 714-717, December 2011.

[17] R. Agarwal, M. S. Santhanam, K. Venugopalan, “Multichannel digital watermarking of color images using SVD,” *IEEE Int. Conf. on Image Information Processing,* pp.1-6, 2011.

[18] S. K. Bhagyashri, M. Y. Joshi, “All frequency band DWT-SVD robust watermarking technique for color images in YUV color space,” *IEEE conf. on Computer Science and Automation Engineering (CSAE),* pp. 295-299, 2011.

[19] C. C. Lai, “An improved SVD-based watermarking scheme using human visual characteristics,” *Int. Journal of Optics Communications,* vol. 284, Issue. 4, 5 pp. 938-944, Feb, 2011.

[20] H. Zhang, H. Shu, G. Coatrieux, J. Zhu, Q. M. J. Wu, Y. Zhang, H. Zhu, L. Luo, “Affine Legendre Moment Invariants for image watermarking robust to geometric distortions,” *IEEE trans. on Image Processing,* vol. 20, no. 8, pp. 2189-2199, Aug, 2011.

[21] H. Song, Z Qiu J. Gu, “A novel semi-fragile image watermarking scheme based on wavelet,” *IEEE Int. Conf. on Audio Language and Image Processing (ICALIP),* pp. 1504-1510, Nov, 2010.

[22] C. C. Lai, “A digital watermarking scheme based on singular value decomposition and tiny genetic algorithm,” *Int. Journal of Digital Signal Processing,* vol. 21 Issue 4, pp. 522-527, July, 2011.

[23] L. Li, W. Y. Ding, J. Y. Li, “A novel robustness image watermarking scheme based on fuzzy support vector machine,” *IEEE Int. Conf. on Computer Science and Information Technology (ICCSIT),* pp. 533 - 537, July, 2010.

[24] R. B. Dili, E. Mwangi, “An image watermarking method based on the singular value decomposition and the wavelet transform,” *IEEE Int. Conf. AFRICON,* pp. 1-5, September, 2007.

[25] H. Qi, D. Zheng, J. Zhao, "Human visual system based adaptive digital image watermarking," *Int. Journal of Signal Processing,* Vol. 88, Issue. 1, pp. 174188, January, 2008.

[26] P. Kapoor, K. K. Sharma, S. S. Bedi, A. Kumar, "Colored image watermarking technique based on HVS using HSV color model," *In Proc. of Int. Conf. on Advances in Computer Engineering,* pp. 20-24, 2011.

[27] R. C. Gonzalez, R. E. Woods, "Wavelet and multiresolution processing," in *Digital Image Processing,* 3^{rd} ed. Ed. India: Pearson Education Inc, pp. 461-524, 2009.

[28] D. Salomon, "Data hiding in images" in *Coding for data and computer communications,* 1^{st} ed. California USA, Springer, pp. 365-415, 2005.

[29] G. Bhatnagar, B. Raman, "A new robust reference watermarking scheme based on DWT-SVD," *Int Journal of Computer Standards & Interfaces,* vol. 31, Issue. 5, pp. 10021013, Sep, 2009.

[30] X. Sun, S. Bo, "A blind digital watermarking for color medical images based on PCA," *IEEE Int, Con. on Wireless Communications, Networking and Information Security (WCNIS),*, pg. 421-427, June 2010.

[31] I. T. Jolliffe, "Introduction," in *Principle Component Analysis,* 2^{nd} ed.Springer, pp. 1-6, 2002.

[32] K. Mahmoud, S.t Datta, J. Flint, "Frequency domain watermarking: An Overview," *Int. Arab Journal of Information Technology,* vol. 2, no. 1, January 2005.

[33] F. Drira, F. Denis, A. Baskurt, "Image watermarking technique based on the steerable pyramid transform," *In Proc. of wavlet application in industrial processing II,* vol. 5607, pp. 165-176, November, 2004.

[34] L. Z. Wing, "Fuzzy rule base and fuzzy inference engine," in *A course in fuzzy systems and Control,* 1^{st}*ed.* Prentice Hall, pp. 90-104, 1997.